UNIVERSITY OF CALIFORNIA

SANTA CRUZ

A VERY HIGH-POWER DENSITY (60-70 kW/kg) SiC INVERTER

A thesis submitted in partial satisfaction

of the requirements for the degree of

MASTER OF SCIENCE

in

ELECTRICAL AND COMPUTER ENGINEERING

by

Joeny Zhen

December 2021

The Thesis of Joeny Zhen

is approved:

_____

Professor Keith Corzine, Chair

_____

Professor Leila Parsa

_____

Professor Yu Zhang

_____

Peter Biehl

Vice Provost and Dean of Graduate Studies

Table of Contents

List of Figures

List of Tables

Abstract

A Very High-Power Density (60-70 kW/kg) SiC Inverter

Joeny Zhen

This thesis describes a very high-power density inverter design for a power train that is intended to be used in an all-electric aircraft. The minimum power density for the power electronics for such an aircraft is 50 kW/kg, but this thesis details designs reaching 60 to even 70 kW/kg, even for a multilevel topology inverter. SiC devices were explored in this thesis because wider bandgap materials such as SiC and GaN can operate at higher temperatures, higher power densities, higher voltages, and higher frequencies – making it the most optimal choice for a long-range all-electric aircraft. This thesis also explored numerous multi-inverter topologies to find the most optimal one for the application – ranging from the typical half-bridge to a neutral-point clamped to even a flying capacitor inverter. Thermal calculations were made only for air-cooling; however, future designs aim for liquid cooling for a longer life-time design. Mechanical bus bar work for a prototype and future designs were made on Onshape and presented here. Additional improvements were explored, ranging from incorporating liquid cooling to an extension to soft-switching. A single-phase prototype was made and experimented. The results are presented in this paper. Currently, I am working on improving the prototype with a next iteration of the design, eventually incorporating it with the motor and thermal designs from other projects.

Acknowledgement

I would like to thank my advisor, Professor Keith Corzine, for providing the financial and educational support in completing the MS degree. His knowledge and expertise have further enhanced my desire to pursue Power Electronics further. In addition, I would like to thank graduate students, Saeid Saeidabadi and Amin Gandomi, for their advice and help in my work. I would also like to thank two undergrads, Joshua McIntire and Joseph Kneeland, for working on smaller tasks associated with my work throughout Summer '21 as I was interning at Lawrence Livermore National Lab. I appreciate all the help and support, thanks!

Chapter 1: *Introduction*

1.1: *Motivation*

In the 21st century, technological innovation suffused over and has greatly improved lives across the world in an unprecedented scale. When encountered with a crisis such as COVID-19, society relied on technological innovation to fast-track numerous vaccinations. Now, we have vaccines from Pfizer, Moderna, J&J, and so on. Companies such as SpaceX have been in the forefront in commercializing space exploration, and innovated methods to improve and lower the cost. Tesla has engaged in decades-long research and development of electric vehicles in the aim of reducing and eliminating the use of fossil fuels. With great technological innovation comes manifested issues. With population becoming denser, energy demand has skyrocketed, resulting in an abundant use of nonrenewable fuels. According to World Energy Production chart by the IEA World Energy Statistics and Balances Group, approximately 80% of the world's energy production is from fossil fuels [1] which generate large amounts of carbon dioxide into the air when combusted. Greenhouse gases such as carbon dioxide trap heat in the atmosphere, which will increase the average global temperature. The Paris Climate Agreement (PCA) aims to hold global temperatures well below 2 degrees Celsius by the next century through intended nationally determined contributions (INDC) that outlines their climate actions. Despite a laid-out plan, it implies a median warming of 2.6 to 3.1 degrees Celsius by

2100. The PCA have quantified the greenhouse gas emissions of the INDC that aims to keep global warming well below 2 degrees Celsius. However, this requires net-zero CO_2 emissions [2].

To obtain net-zero CO_2 emissions, technological advancements are adamantly required. From the listed well-known technological advancements, Tesla has been in the forefront in reducing and eliminating the use of fossil fuels in the transportation sector through their research and development of electric vehicles. According to the US EPA, the transportation sector accounts for 28% of greenhouse gas emissions in the US where nearly 60% comes from light-duty/passenger vehicles [3]. To get a better idea of how EVs will improve and reduce global warming, a study was made in Germany by Schill and Pruckner et al., disclosing the potential impact of a high number of EVs on Germany's energy system. If six million EVs are in Germany's transportation system, it is expected greenhouse gases will be reduced by 37% in comparison to a situation where there are no EVs on the road [4].

Years of research and development has focused on the need reduce and eliminate fossil fuels in the automobile industry, but it accounts for 60% of transportation in the US. Approximately 30% of greenhouse gas emissions from transportation are from medium-heavy duty vehicles and aircraft. More R&D must be carried out in these sectors to achieve net-zero CO_2 emissions. With a *very real* fear of global warming's ramification on the world and the need for net-zero CO_2 emissions, *I am motivated and determined* to research this further.

1.2: *Mission*

Medium-heavy duty vehicles and aircraft, similar to the current electric vehicles, consist of a power train: the electric motor, the drive, and the thermal management system. The difference in requirement is to have enough power density to drive typical loads one would see during off-road applications or long-range flight. Thus, innovative designs are required to achieve an ultralight high power-dense system. Recently, a team led by Leila Parsa and Keith Corzine received funding by the US DOE to develop an all-electric power train for a future aircraft, similar to the Boeing 747, however, the current electric power trains do not have enough power density and efficiency to meet the requirements. An all-electric aircraft is needed because the carbon dioxide emissions per passenger from commercial aircraft are approximately double of any other form of transportation. The goal is to reduce emissions from commercial air travel [5].

The mission of this thesis is to detail the current research and development findings for the drive, also known as the power electronics of the design. The drive of the system is an inverter that aims to achieve a power density of at least 50 kW/kg. High efficiency and lower EMI are obtained by using state-of-the-art multilevel inverter technology and Silicon Carbide (SiC) devices.

1.3: *Related Works*

With regards to designing an all-electric aircraft, there have been some efforts made in designs, including improving the power systems and the power electronics section of the aircraft. In [6], a converter was made to have a power density of 19 kW/kg with 99% efficiency with a non-cryogenic cooling system, and a power density of around 26 kW/kg with a cryogenic cooling system and identical efficiency. In another paper, [7], a power density of 30 kW/kg for its switching converter was achieved. However, for the intended application of long-range flight similar to the Boeing 747, a power density of 50 kW/kg is required.

From literature, there has been some effort made to design a very high-power density inverter using SiC devices and multi-level design. In [8], a power density of 50 kW/kg was achieved by the following removing the body diodes from the modules, using a two-level half-bridge topology, and developing a high performing gate driver. In [9], a power density of 50 kW/kg was also achieved, and very similar steps were made compared to [8]. However, the researchers did not remove the body diodes from the modules. The biggest difference between [8] and [9] is their choice of cooling design. In [8], they decided to use a copper-based heatsink with forced air convection. While in [9], they use a liquid-cooled heatsink. As a note, both papers implemented the half-bridge two-level topology. The design of the inverter this thesis entails is influenced by the related works discussed.

Chapter 2: *Simulation*

2.1: *Overview*

The main objective of the three-phase inverter design is to have a power density of at least 50 kW/kg at 97% efficiency or higher. The minimum output power level is 250 kW. Before going into the design, numerous topologies were simulated to get a better idea of the electrical performance of the inverter, namely:

1. Two-Level Half-Bridge Inverter
2. Three-Level Flying Capacitor Inverter
3. Three-Level Neutral Point Clamped Inverter
4. Four-Level Flying Capacitor Inverter

The following sections detail the designs of these topologies

2.2: *Two-Level Half-Bridge Inverter*

In this design, the inverter is connected to a permanent-magnet ac motor [21] and 1200V MOSEFET semiconductors are used. Figure 1 shows the Simulink simulation diagram. The parameters and operating conditions are:

Parameters and Operating Conditions

P = 8	r_S = 19.3 mΩ	L_s = 300 µH	λ'_m = 0.19 Vs
V_{dc} = 900 V	w_{rm} = 5000 rpm	d = 1.074	
V_S = 342 V	φ_v = 33.1 deg		
I_S = 297 A	φ_i = 0 deg		

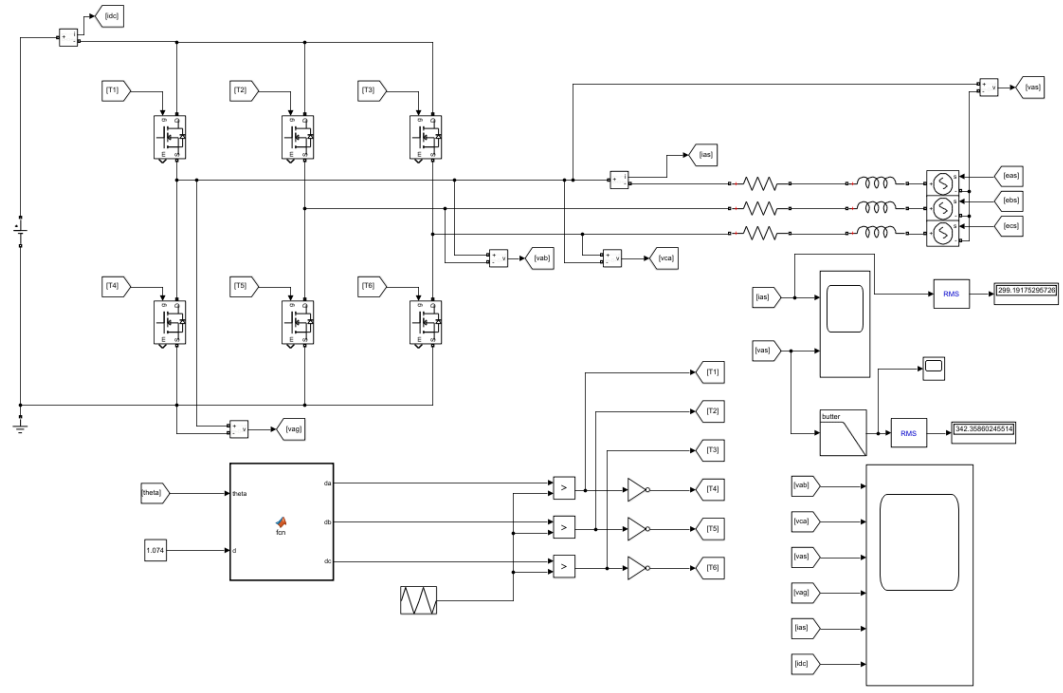

Figure 1. Two-Level Half-Bridge: *Inverter* Section MATLAB Simulink Schematic

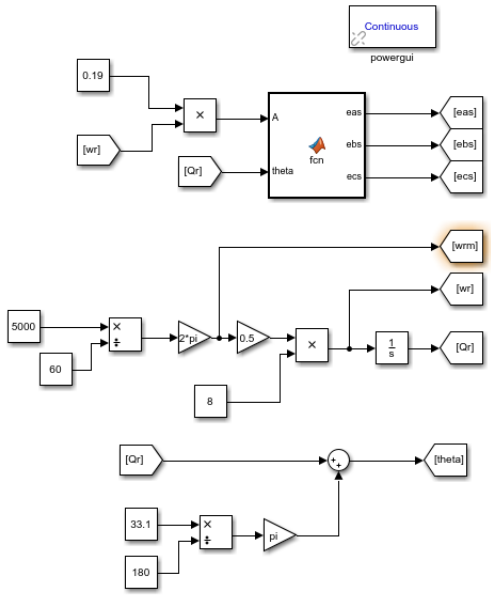


```
1    function [eas, ebs, ecs]= fcn(A, theta)
2 -    eas = A*cos(theta);
3 -    ebs = A*cos(theta-((2*pi)/3));
4 -    ecs = A*cos(theta+((2*pi)/3));
5
```

Figure 2. Two-Level Half-Bridge: *Motor* Section MATLAB Simulink Schematic

From the Figure 1, the current, Ias, is 299 Arms, and the voltage, Vas, is 342 Vrms, which results in a total power of 307 kW. The desirable power is a minimum of 250 kW.

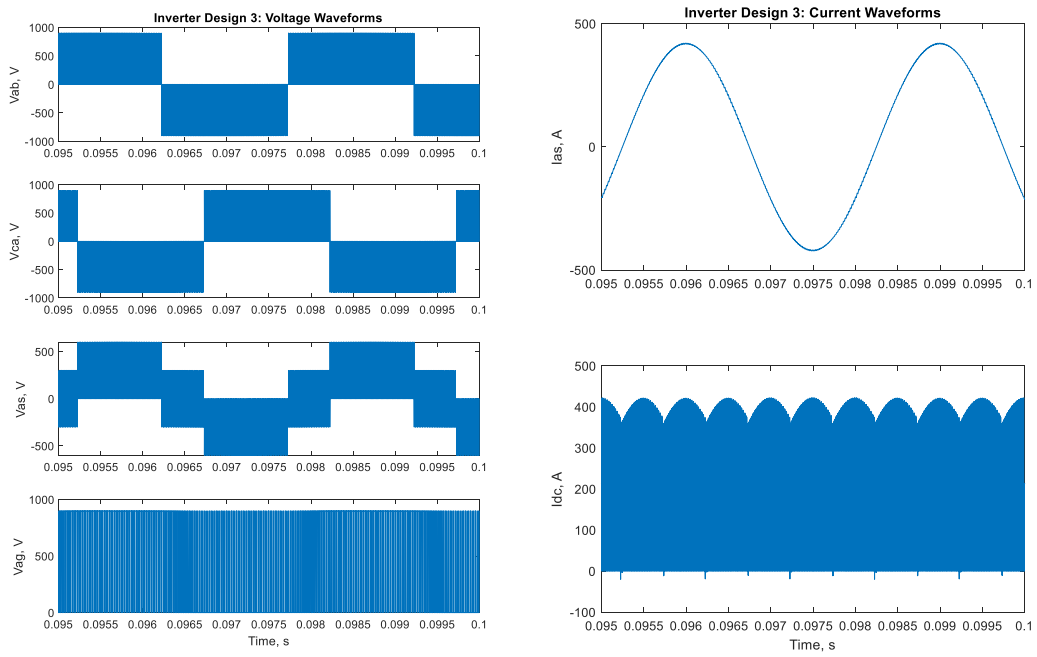

Figure 3. Two-Level Half-Bridge Inverter Voltage and Current Waveforms

From Figure 1, the two-level half-bridge inverter implements sine-triangle modulation for the switching states. The inverter is connected to a permanent-magnet synchronous motor, where the parameters are established in Figure 2. The back EMF is done through using the MATLAB function block, which outputs to a voltage-dependent voltage source for each phase: Eas, Ebs, and Ecs. The back EMF of a PMSM is established based on the following equation:

$$E_{as} = \lambda'_m \omega_r \cos(\theta) \quad (1)$$

$$\omega_r = angular\ velocity\ of\ the\ rotor \quad (2)$$

$$\lambda'_m = flux\ induced\ by\ the\ PM\ of\ the\ rotor\ in\ stator\ phases \quad (3)$$

2.3: *Three-Level Flying Capacitor Inverter*

This simulation consists of the following parameters when using 1200V devices:

Parameters and Operating Conditions

P = 8 Poles	r_S = 77.2 mΩ	L_s = 300 µH	λ'_m = 0.379 Vs
V_{dc} = 1800 V	w_{rm} = 5000 rpm	d = 0.912	
V_S = 580 V	φ_v = 9.3 deg		
I_S = 148 A	φ_i = 0 deg		

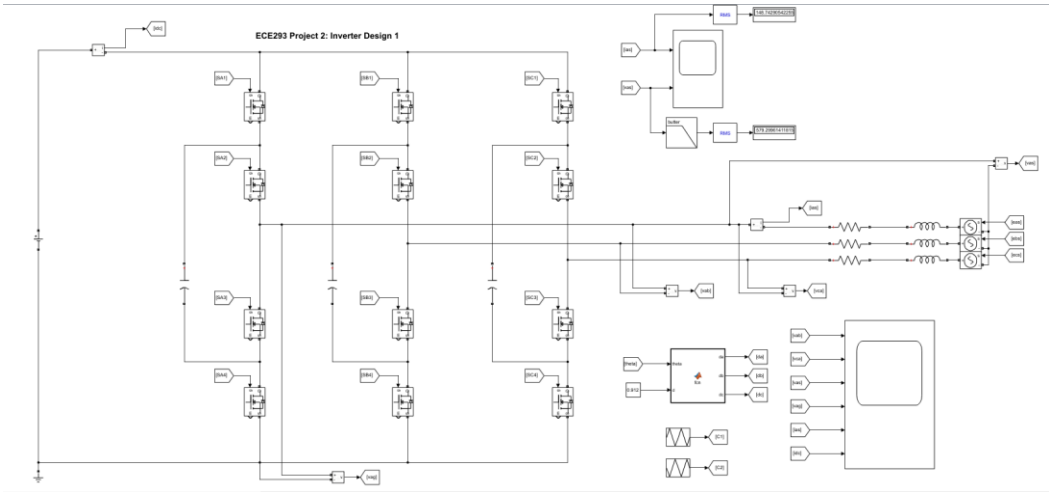

Figure 4. Three-Level Flying Capacitor: *Inverter* Section MATLAB Simulink Schematic

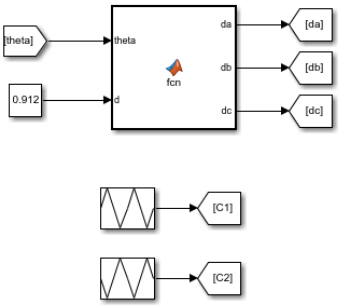


```
function [da, db, dc]= fcn(theta, d)

da = d*cos(theta) - (d/6)*cos(3*theta);
db = d*cos(theta - (2*pi/3))- (d/6)*cos(3*theta);
dc = d*cos(theta + (2*pi/3))- (d/6)*cos(3*theta);


```

Figure 5. Three-Level Flying Capacitor: PS-PWM Implementation

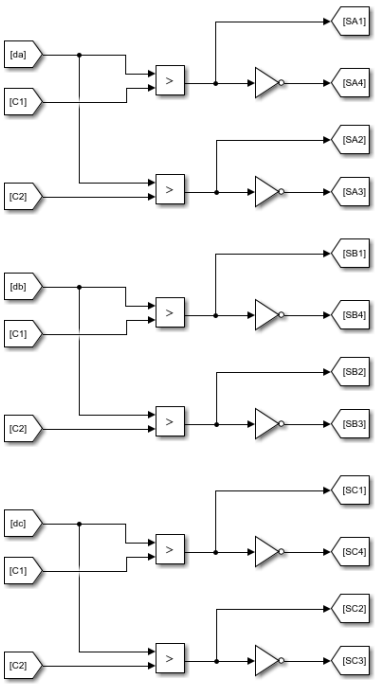

Figure 6. Three-Level Flying Capacitor: Switching States

Phase-shifted pulse-width modulation (PS-PWM) is implemented by phase shifting the triangle wave compared to its base refence by 360 degrees/(# of levels - 1). The benefit of using PS-PWM in a FCI is its ability to naturally balance the capacitor voltage to Vdc/(# of levels – 1) in multi-level FCI topologies. In this case, the balanced voltage is 900V across the capacitor [10].

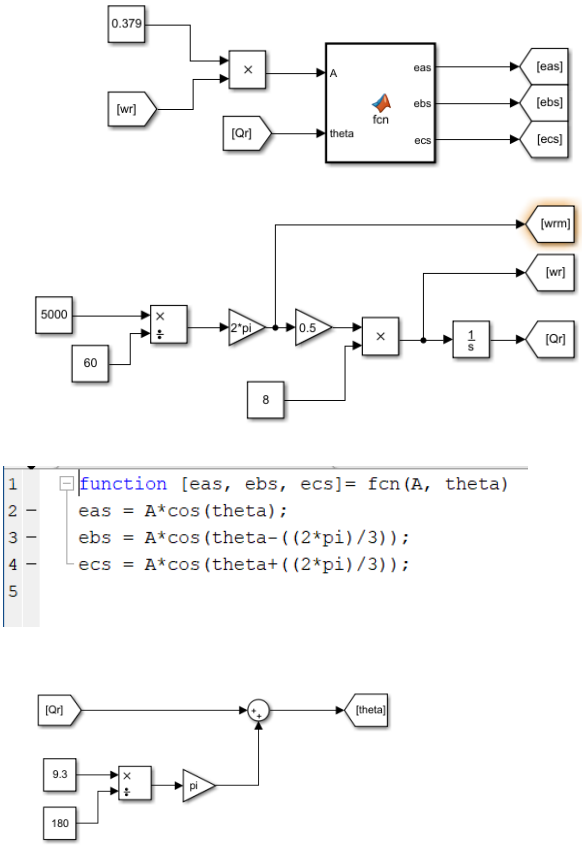

Figure 7. Three-Level Flying Capacitor: *Motor* Section MATLAB Simulink Schematic

From Figure 4, the current, Ias is 149 Arms, and the voltage, Vas, is 580 Vrms, which results in a total power of 259 kW.

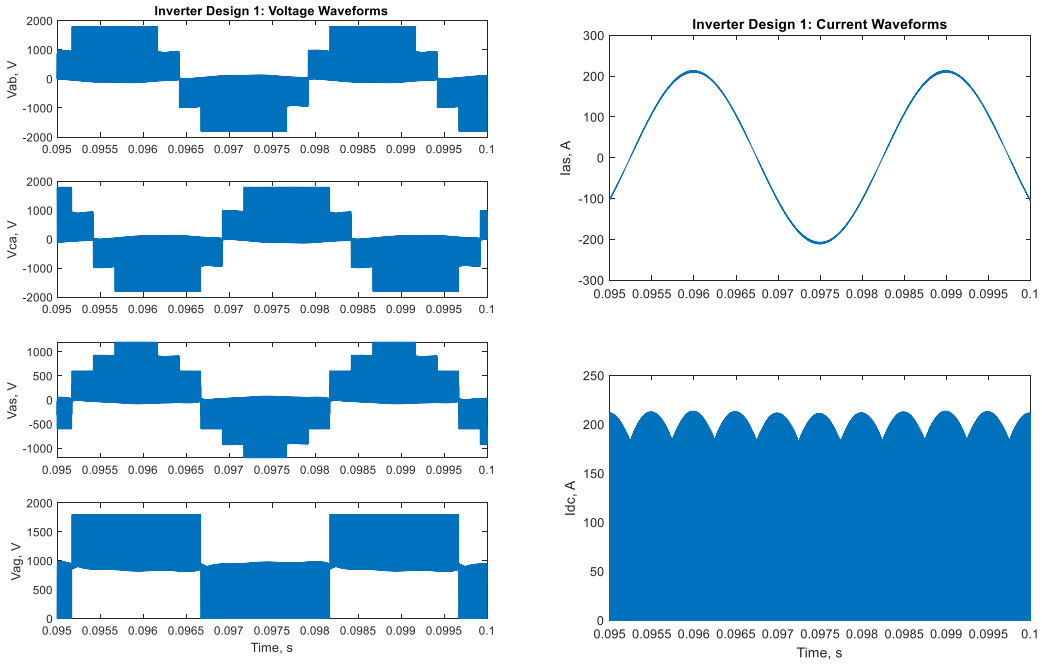

Figure 8. Three-Level Flying Capacitor Inverter Voltage and Current Waveforms

The implementation of the permanent-magnet motor is identical in the two-level half-bridge simulation as seen in Figure 7.

2.4: *Three-Level Neutral-Point Clamped Inverter*

The parameters for the Three-Level NPC are identical to the Three-Level FCI.

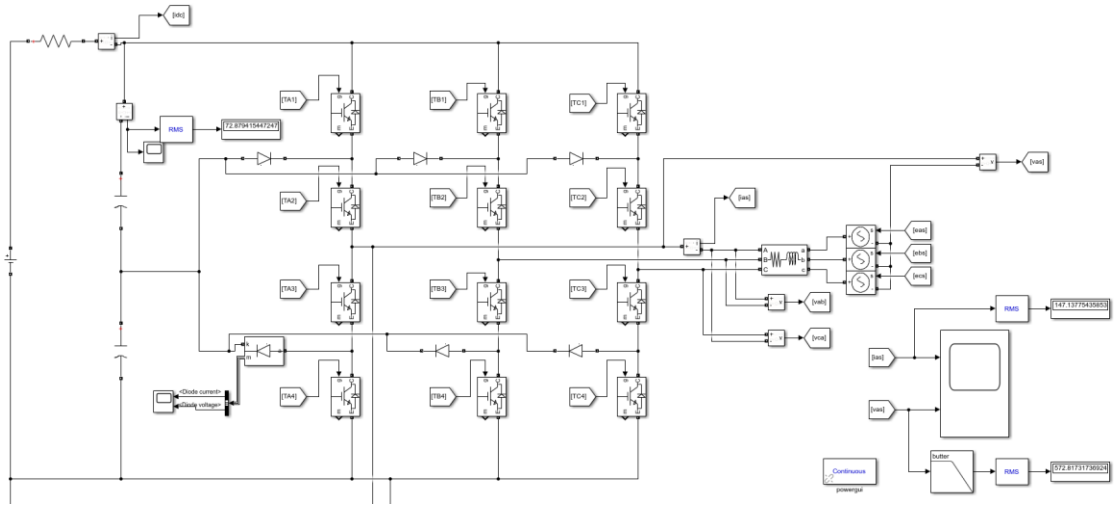

Figure 9. Three-Level Neutral Point Clamped: *Inverter* Section MATLAB Simulink Schematic

The motor section of the three-level NPC simulation is identical to the one shown in section 2.2 and 2.3.

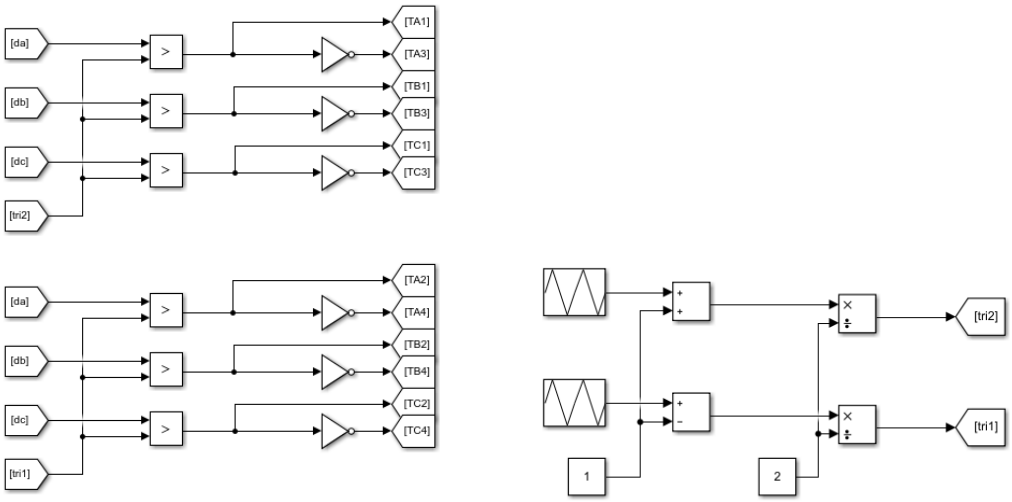

Figure 10. Three-Level NPC Switching States and PD-PWM Implementation

Phase-deposition pulse-width modulation (PD-PWM) is used due to its ability to reduce high frequency THD in multi-level NPC topologies [11].

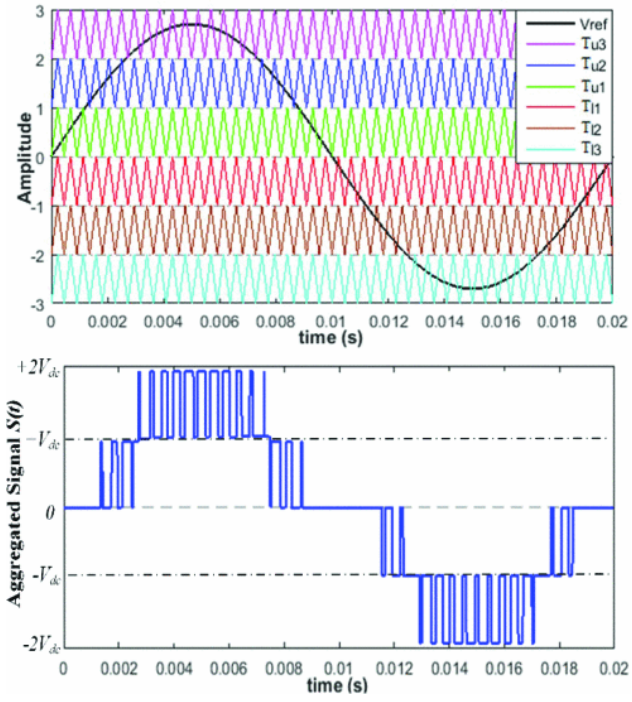

Figure 11. PD-PWM Implementation Example [11]

To implement PD-PWM, first, the number of triangle waves required is determined by # of levels -1. As seen in Figure 11, to implement PD-PWM, the triangle waves are stacked on top of each other within the amplitude range of the sine wave. From Figure 9, the current and voltage is the same as the Three-Level FCI simulation, resulting in a power output of 259 kW.

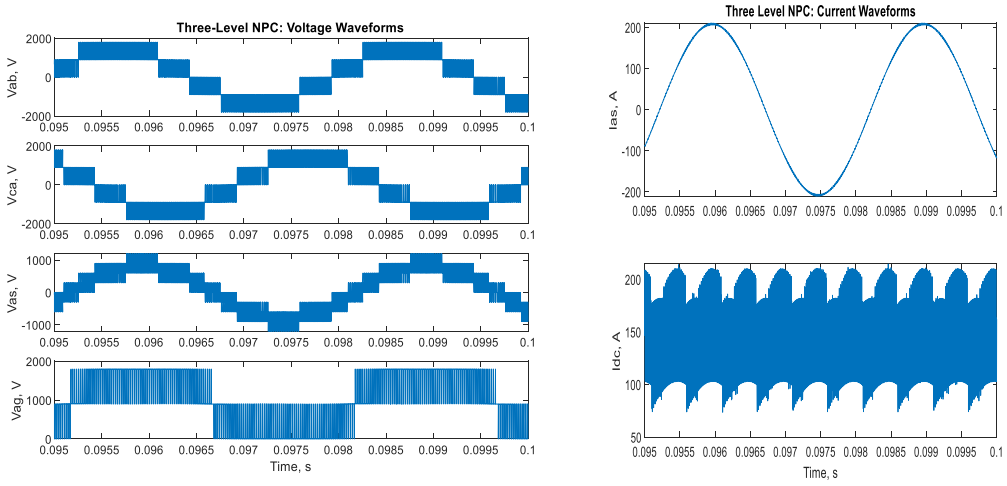

Figure 12. Three-Level NPC Voltage and Current Waveforms

2.5: *Four-Level Flying Capacitor Inverter*

This simulation consists of the following parameters when using 1200V devices:

Parameters and Operating Conditions

P = 8 Poles	r_S = 35 mΩ	L_s = 300 µH	λ'_m = 0.58 Vs
V_{dc} = 2700 V	w_{rm} = 5000 rpm	d = 0.912	
V_S = 870 V	φ_v = 4 deg		
I_S = 100 A	φ_i = 0 deg		

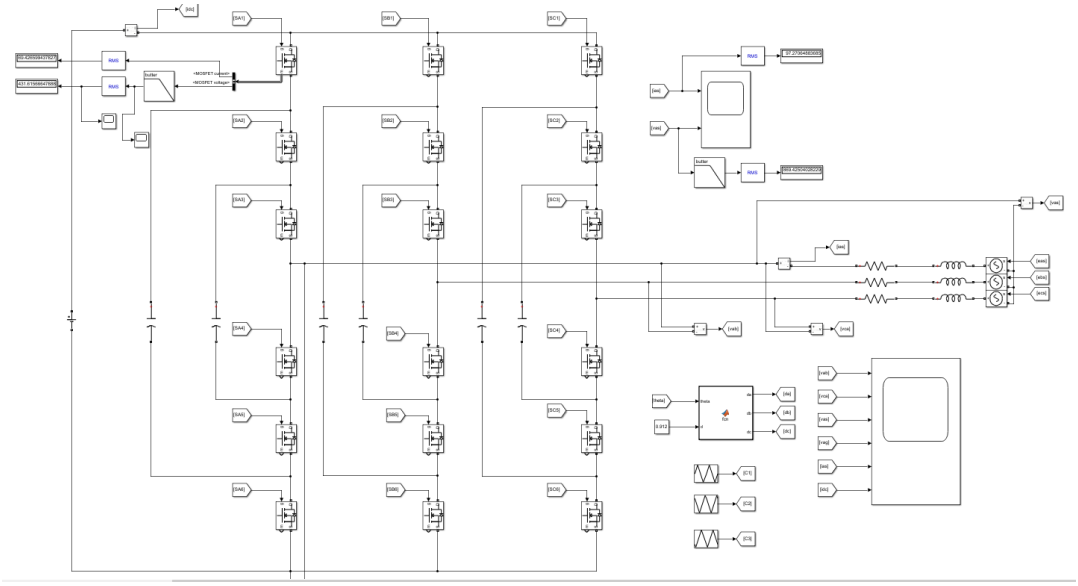

Figure 13. Four-Level Flying Capacitor: *Inverter* Section MATLAB Simulink Schematic

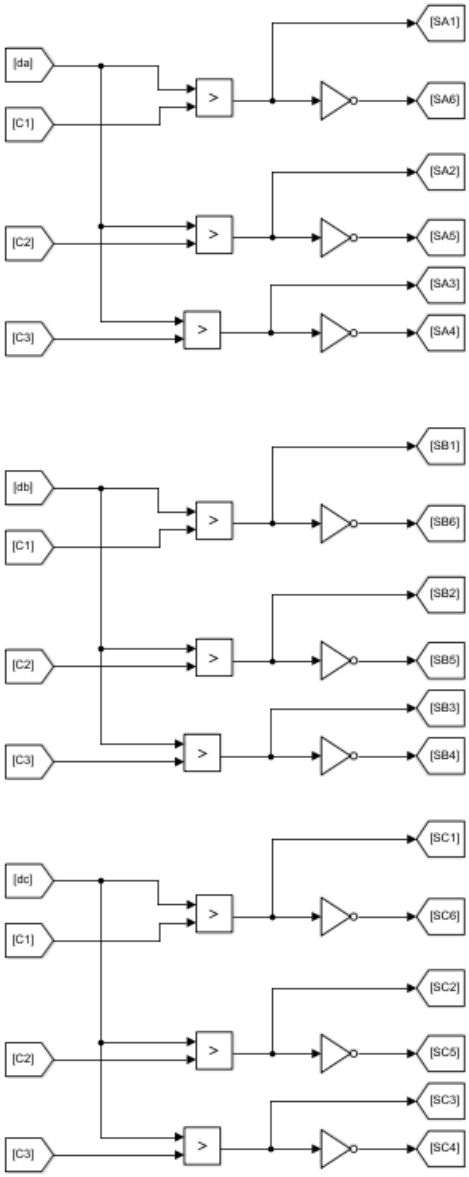

Figure 14. Four Level FCI Switching States

The motor section of the simulation is identical section 2.2 and 2.3. From Figure 13, the current, Ias, is around 98 Arms, and the voltage, Vas, is 870 Vrms, which results in a total power of 256 kW.

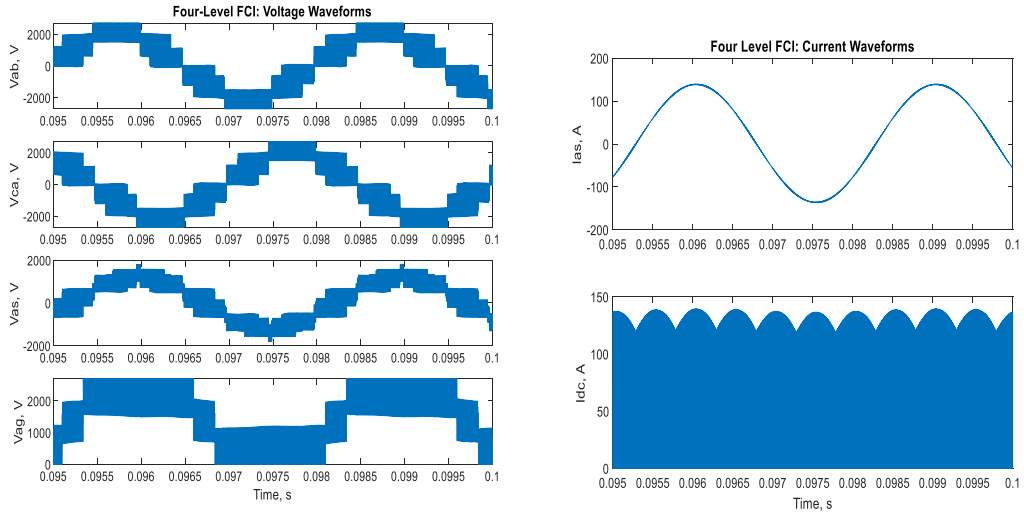

Figure 15. Four Level FCI Voltage and Current Waveforms

2.6: *Topology Selection*

Choosing a reasonable topology is vital when it comes to satisfying the power density requirement of 50 kW/kg. Different topologies have different weights due to the required components. The two-level half-bridge will result in the lightest design due to its simplicity. However, its efficiency and EMI is a lot worse in comparison to multi-level topologies. It is logical to select a higher-level topology for the design. Thus, the two-level half-bridge can be used as a last resort if problems arise.

This leads to a selection amongst the other three listed topologies. Provided that a minimum power density of 250 kW/kg is required and an output power of 50 kW, the maximum weight the inverter must be is 5 kg. The downside of implementing higher multilevel topologies is the additional weight due to the additional switches. The lightest module (half-bridge) found on the marketplace is

from CREE (the HM3 and XM3 families). The weight of these modules is approximately 180g each. However, its gate driver and differential transceiver add an additional 100g. Provided that in a four-level topology requires 18 switches in total (9 half-bridges), the weight of the modules total to 2520g. The four-level power density can be investigated.

The selection amongst the remaining topologies was done through comparing the weight between the flying capacitor and the diode in the NPC. Generally speaking, a ceramic based capacitor is significantly lighter than the typical bulky power diodes seen in the market, thus, the three-level FCI was chosen for the design.

Chapter 3: *Weight*

3.1: *Overview*

The composition of any inverter design is the following: semiconductor devices, gate drivers, heatsink, busbar connections, fans/liquid cooling, connectors, and capacitors/diodes. The selection of these components is done to satisfy voltage and current requirements, and to not exceed the thermal junction temperature of the modules. This is all done while keeping the weight as low as possible to maximize the power density of the inverter.

3.2: *Module Selection*

The chosen topology for the design is the three-level flying capacitor inverter. This requires a total of 12 switches, or 6 half-bridge modules. According to the simulation done in section 2.3, the current requirement is 148 Arms using 1200V devices. There are many devices composed of different semiconductor material such as Si, SiC, and GaN can satisfy the electrical requirements. However, different semiconductor materials can have a significant impact on the weight and efficiency performance.

Wider bandgap materials such as SiC and GaN can operate at higher temperatures, higher power densities, higher voltages, and higher frequencies, making these the best semiconductor choice selection for the inverter design instead of Si. For high power applications where power density is a paramount requirement, SiC is the best choice due to its higher thermal conductivity of around 5 W/cmK versus GaN's measly 1.3 W/cmK. This allows designers to select a significantly lighter heatsink for SiC devices instead of GaN for the same amount of losses.

Searching through the marketplace such as Digikey and Mouser resulted in the following choices for the module:

1. CREE HM3 1200V/760A: CAB760M12HM3
2. CREE HM3 1200V/480A: CAS480M12HM3
3. CREE XM3 1200V/450A: CAB450M12XM3

The thermal performance and total weight of the design is based on the three listed choices. The weight of the 'HM3' modules is 180g. The weight of the 'XM3' modules is 175g.

3.3: *Gate Drivers and Differential Transceiver*

The selected modules for the design all have designed gate drivers to its corresponding 'family' type. For modules 1 and 2, they are classified as the 'HM3' family and the corresponding gate driver for this family is CGD1700HB3P-HM3 as shown in Figure 16. The weight of this gate driver measures around 70g.

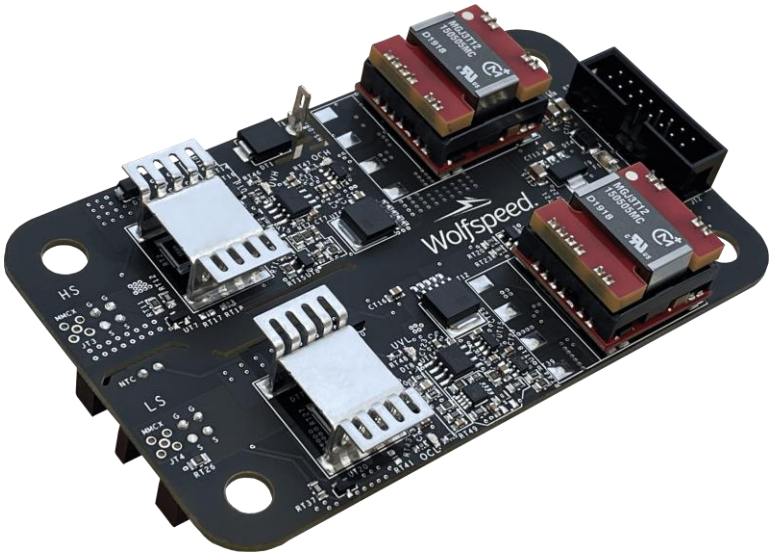

Figure 16. Gate Driver (CGD1700HB3P-HM3) for the HM3 Family

For module 3, it is classified as the 'XM3' family, which is a different type of package, and the corresponding gate driver for this module is CGD12HBXMP as shown in Figure 17. The weight of this gate driver measures around 40g.

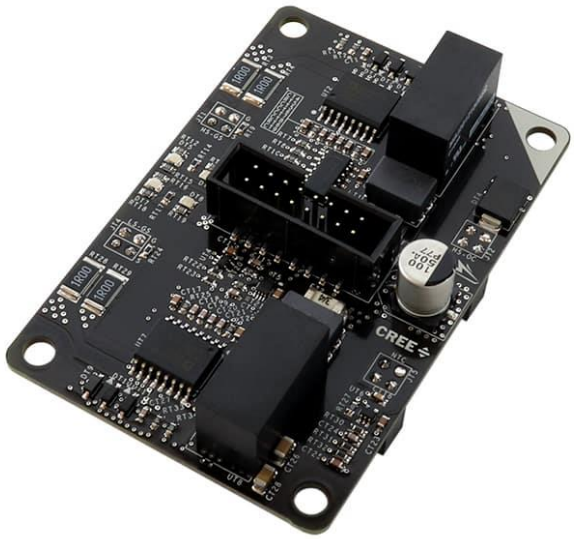

Figure 17. Gate Driver (CGD12HBXMP) for the XM3 Family

Both gate drivers shown in Figures 16 and 17 accept differential signals. However, when controlling them with a DSP which is a very common strategy, DSP outputs a single-ended type signal. Therefore, some sort of 'converter' is required to integrate a DSP to the gate driver. CREE offers something called a differential transceiver which converts a single-ended input to a differential output. Figure 18 displays a block diagram detailing how it should be wired. Figure 19 provides a real physical example of how it is done using the 'HM2' or 'HM3' family modules. The weight of the differential transceiver is around 25g.

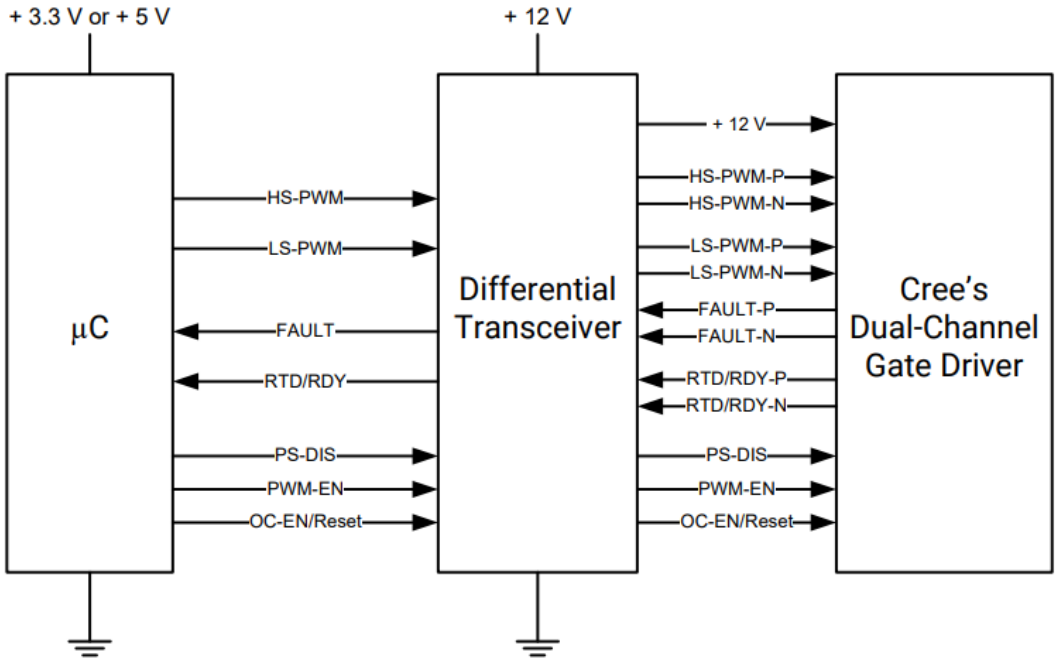

Figure 18. Block Diagram of Inverter Signal Chain [12]

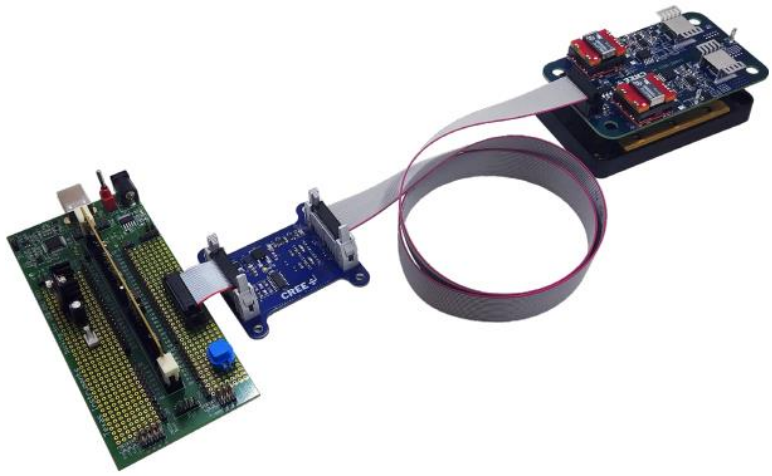

Figure 19. Example of Inverter Signal Chain [12]

3.4: *Flying Capacitor*

The selection of the capacitors for the FCI was chosen based on the weight, voltage, and current requirements. Generally speaking, ceramic based capacitors are significantly lighter than electrolytic based for high power applications. The capacitance used in the simulation was 2 µF. The following capacitor was used for the initial prototype as seen in Figure 20: L1GN40D274KA05. The capacitor is rated for 2000V and around 10-15 Arms. Each capacitor is 0.2 µF worth of capacitance. The weight of these capacitors is around 10g each. To achieve 2 µF and reduce the current load through each capacitor, 10 of these capacitors were placed in parallel. The total weight of the capacitors is around 100g.

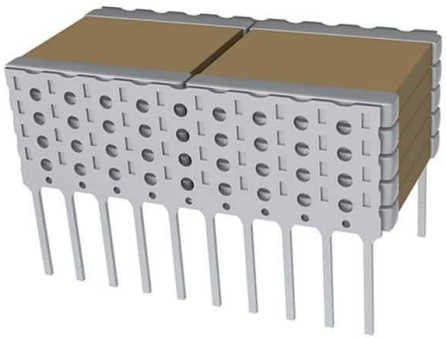

Figure 20. Ceramic Capacitor used for FCI

3.5: *Heatsink*

For dissipating the heat from the inverter, either a heatsink or a coldplate is required. A heatsink can implement either natural or forced convection. A coldplate is used to cool down the inverter more efficiently through liquid cooling. For a prototype, it is easier to implement a heatsink and air cooling with a fan instead of liquid cooling where a coldplate, coolants, pumps, and more are required. For a more future design, it would be wise to use liquid cooling to maintain the temperature of the inverter at a low to maximize the lifetime of the design.

The selection of the heatsink is entirely dependent on how well the thermal performance limits the temperature within the maximum junction temperature of the module. According to each of the datasheets, the maximum junction temperature of the modules is 175 degC.

$T_{VJ\,op}$	Maximum Virtual Junction Temperature under Switching Conditions	-40		175	°C	

Figure 21. Maximum Junction Temperature of Chosen SiC Modules [13]

Heatsink Design 1 (CAB760M12HM3): 3-Level FCI Topology

Total temperature performance is calculated by the four thermal conduction parameters.

Thermal Conduction Resistance Between Junction and Case (MOSFET)

Thermal Conduction Resistance Thermal Conductor (Thermal Adhesive)

Thermal Conduction Resistance Heatsink

Thermal Conduction Resistance Ambient, Assume Room Temperature (25 degC)

According to the datasheet, the maximum thermal resistance junction-to-case for the MOSFET is R_{thJCM} = 0.073 degC/W. The maximum junction temperature is 175 deg C [13].

$$R_{TH\_JCM} = 0.068\ {}^{degC}/_{W} \text{ (for 1 a module)}$$

$$R_{TH\_JCM} = 0.0226\ {}^{degC}/_{W} \text{ (for 6 modules typical)}$$

Expected Power Loss by the Switches: $12[(148A)^2*(0.00173\ \Omega)] = 349.59W$

Maximum Junction Temperature: 175 degC.

Maximum Thermal Resistance: $\frac{175-25}{349.59} \approx 0.43\ degC/W$

Chosen Thermal Adhesive: Wakefield-Vette (GL-60-10)

The terminal resistance of a material is calculated with the following equation:

$$R_{cond} = \frac{L}{kA} \; in \; units \; of \; {}^{degC}/_{W}$$

Where L is thickness in meters, k is the thermal conductivity of the material in (W/K*m), and the cross-sectional area (m^2).

The application thickness of this adhesive is assumed to be 0.5mm. The minimum application area is 44900 mm^2 = 0.0429 m^2. The thermal conductivity of the adhesive is 3 W/m-K. The thermal resistance of the thermal adhesive is:

$$R_{TH\_TA} = \frac{0.5*10^{-3}m}{(3 \; {}^{W}/_{m-K})(0.0429 \; m^2)} = 0.0039 \; {}^{degC}/_{W} \text{ (for all 6 modules)}$$

$$R_{TH\_TA} = 0.0234 \; degC/W \; (per \; module)$$

<u>Maximum Heatsink Thermal Resistance</u>: 0.43-0.0113-0.0039 = 0.4148 degC/W (Single)

For all six modules, the maximum thermal resistance of the heatsink is 0.4148*6 = 2.4888 degC/W. It would be wise to use a heatsink with a thermal resistance a bit lower than maximum.

The area of a single module is 65mm x 110mm = 7150 mm^2 = 11.083 in^2. For a three-level, three-phase flying capacitor-based inverter, 6 modules are required. The total minimum area required to have all 6 modules on a heatsink is 42900 mm^2 = 66.5 in^2.

If the modules are laid out in a 2-by-3 array, the minimum length is 110x2 = 220 mm. The minimum width is 65x3 = 195 mm.

If the layout is a 3-by-2 array, the minimum length is 110x3 = 330 mm. The minimum width is 65x2 = 130 mm.

If the layout is a 1-by-6 array, the minimum length is 110 nm. The minimum width is 65x6 = 390mm. If the layout is a 6-by-1 array, the minimum length is 110x6 = 660mm. The minimum width is 65mm.

Using a layout of 3-by-2, the chosen heatsink is Aavid Thermalloy (688552F00000G) [14]

Heatsink Dimensions (assuming a module layout of 3x2) (Heatsink needs to be cut):

Length: 330 mm (Heatsink Minimum Length Cut)

Width: 182.9 mm

Height: 12.83 mm

Over Area: 60357 – 42900 = 17457 mm^2

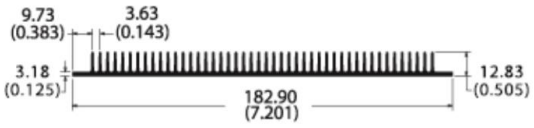

68855 PRODUCT DETAILS

Property	Details
Height	.505 in (12.83 mm)
Width	7.201 (182.90 mm)
Perimeter	46.30 in
Weight	1.7 lb per foot (2.53 kg per meter)
Material	6063-T5 Aluminum Extrusion Alloy

Figure 22. Aavid Thermalloy (688552F00000G) Physical Parameters [14]

Heatsink Weight: 2.53 kg per meter (length)

Ideal Weight: $2.53\ {}^{kg}/_{m} * \frac{330\,mm}{1000mm} * 1m = 834.9g$

Thermal Resistance (Natural Convection): Around 1.5 degC/W

Thermal Resistance (at 100 LFM): 1.12 degC/W

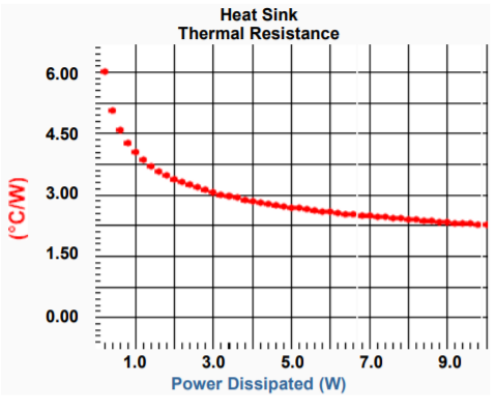

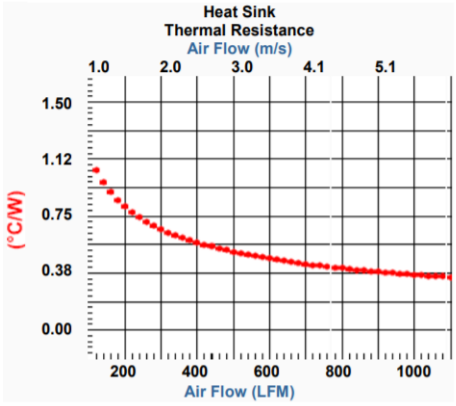

Figure 23. 688552F00000G Thermal Resistance at Natural (L) and Forced Convection (R) [14]

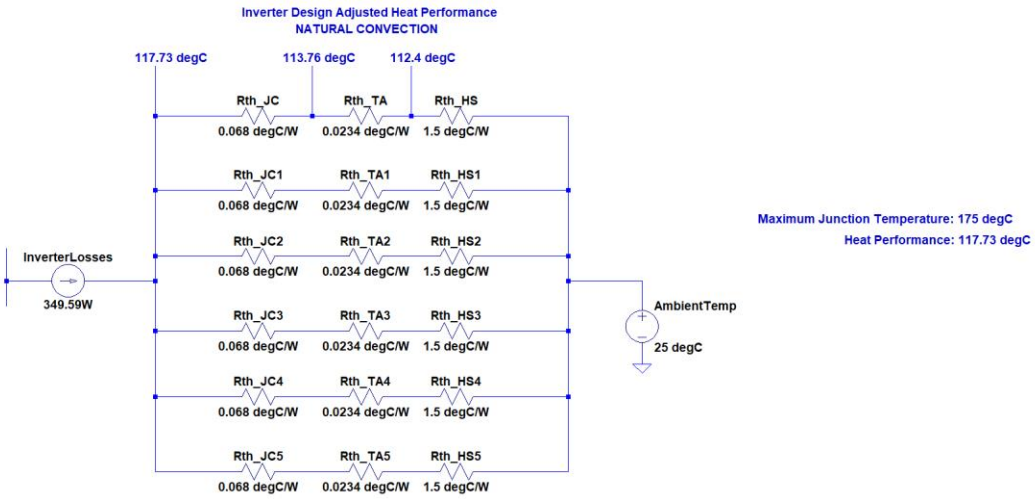

Figure 24. FCI Design (CAB760M12HM3) at Natural Convection

From the best identified switch and a chosen heatsink (688552F00000G), the weight of the heatsink comes out to be 835g with a junction temperature performance of 117.73 degC using natural convection.

Second Heatsink Design (CAS480M12HM3): 3-Level FCI Topology

Identical steps were made in this section when determining the weight of the heatsink and the junction temperature performance.

For the chosen switch, CAS480M12HM3, the same heatsink is used provided the package is the same as the first heatsink design. The difference between two switches are its electrical and thermal resistance values. For CAS480M12HM3, the electrical resistance is 2.3 mΩ and its thermal resistance is 0.1 degC/W [15]. For the first heatsink design, the electrical resistance is 1.33 mΩ and its thermal resistance is 0.068 degC/W. Unfortunately, the second heatsink design switches do require some sort of forced convection provided its electrical and thermal resistances cannot keep the junction temperature low enough during natural convection. Figure 25 displays a schematic detailing the thermal performance of CAS480M12HM3 with an airflow of 400 LFM.

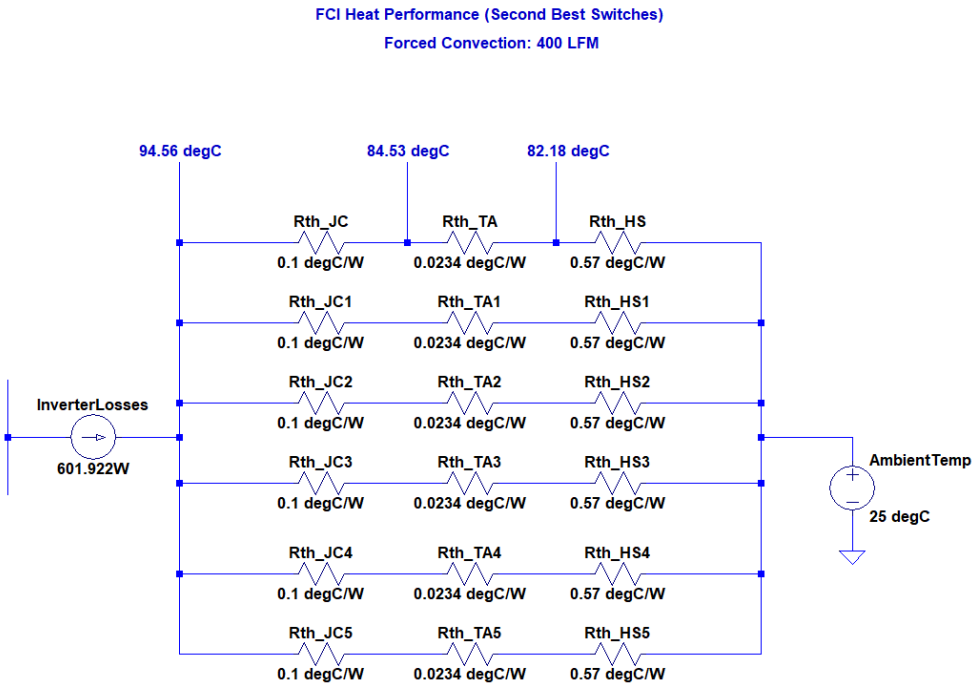

Figure 25. FCI Second Switches (CAS480M12HM3) Thermal Performance at 400 LFM Airflow

The thermal performance of second heatsink design switches from the 'HM3' family with an airflow of 400 LFM results in a junction temperature of 94.56 degC. The weight of the heatsink is identical to the best switches design of 835g.

Third Heatsink Design (CAB450M12XM3): 3-Level FCI Topology

For the 'XM3' family, its electrical and thermal resistances are quite similar to its 'HM3' counterpart. According to the datasheet of the selected 'XM3' module (CAB450M12XM3), the electrical and thermal resistances are 2.6 mΩ and 0.11 degC/W respectively [16]. The dimensions of these modules are a tad smaller, allowing for a lighter heatsink.

If the modules are laid out in a 2-by-3 array, the minimum length is 80x2 = 160 mm. The minimum width is 53x3 = 159 mm.

If the layout is a 3-by-2 array, the minimum length is 80x3 = 240 mm. The minimum width is 53x2 = 106 mm.

If the layout is a 1-by-6 array, the minimum length is 110 nm. The minimum width is 53x6 = 318mm. If the layout is a 6-by-1 array, the minimum length is 80x6 = 480mm. The minimum width is 65mm.

By using a layout of 2x3 and the same heatsink as the previous designs shown in Figure 22, the weight of the heatsink is 402.3g, cutting the heatsink weight by half. Due to its similar electrical and thermal resistances, the heat performance is the same as the second-best 'HM3' design. The junction temperature of this design will also result in 94.56 degC as seen in Figure 25.

Fourth Heatsink Design (CAB760M12HM3): 4-Level FCI Topology

A four-level FCI topology was investigated to identify the highest possible level the selected modules can achieve while maintaining a minimum power density of 50 kW/kg. By going through identical steps as shown previously, Figure 26 displays the junction temperature performance of a four-level FCI design using the 'HM3' module rated for 760A. A natural convection, the expected junction temperature is around 77 degC. The total weight of the heatsink, due to an additional 3 modules expanding its area, is 910.8g.

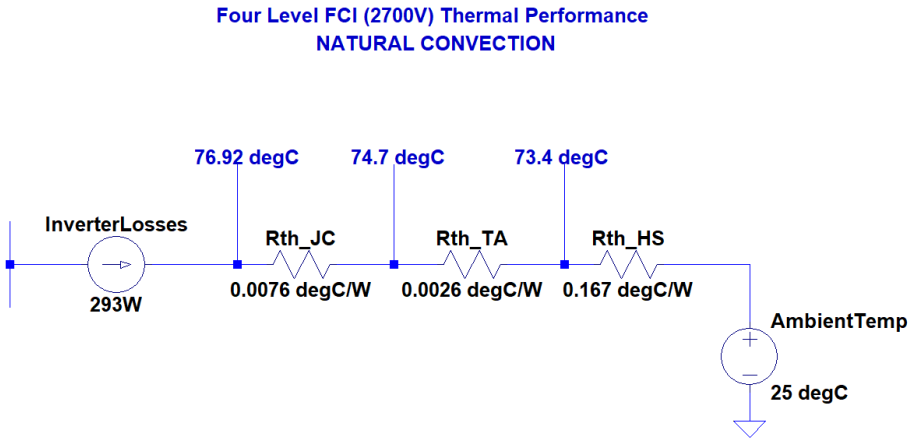

Figure 26. Four Level FCI (CAB760M12HM3) Junction Temperature at Natural Convection

3.6: *Busbar*

Busbar work is required to form the necessary connections between each junction. Similar to a PCB, layers were made to form the necessary electrical connections: a VDD layer, a ground layer, and signal layers. The selection of the busbar material was limited to either copper or aluminum due to its abundancy. Provided that the primary objective of the inverter design is to maximize out its power density, aluminum was chosen as the bus bar material due to its density being significantly lower than copper:

$$\text{Cu (density)} = 8.96\ \text{g/cm}^3$$

$$\text{Al (density)} = 2.7\ \text{g/cm}^3$$

The prototype bus bar work was developed for the Three-Level FCI design that implements the modules from the 'HM3' family. The area of the bus bar connections was formulated from the following logic:

- The length must span within the length of the modules = 70 mm
- The width must span around 2.5x the width of the modules = 150 mm
    - It must contain both modules within the width of the bus bar

Similar to PCBs where larger copper trace sizes are required to carry the necessary current, large busbar work is required to carry the necessary current of the inverter. This determines the height of the busbar work. Unfortunately, there is a tradeoff between using aluminum versus copper. Aluminum has a current density lower than

copper by a factor of a 1.6/1 ratio. The current density of copper is generally 500 A/cm^2. Therefore, the current density of aluminum is around 500/1.6 = 312.5 A/cm^2. Despite a lower current density, the tradeoff between weight and current density is still beneficial for the design when minimizing weight. Therefore, the minimum cross-sectional area is:

$$150\ Arms/(312.5\ A/cm^2) = 0.48\ cm^2 = 48\ mm^2$$

Provided the current flow is facing into the length's edge (70 mm) of the busbar, the height must be at least:

$$48\ mm^2/70mm = 0.69\ mm = 0.03\ inches$$

For the prototype, a height of the bus bar was selected to be 0.1 inches to mitigate any potential electrical problems or issues due to the material selection while minimizing the weight of the design.

Figures 28-31 provides a figure of the bus bar design for each layer of the inverter. The design of the bus bar was created in a free CAD tool called Onshape. Smaller holes are present to form an electrical connection between the aluminum plane to its corresponding point and screws. Larger holes serve as clearance to prevent screws touching other layers unintentionally. Midsized holes are done for clearance of the screw's thread. Each layer is separated by fiberglass insulation rated for 3 kV.

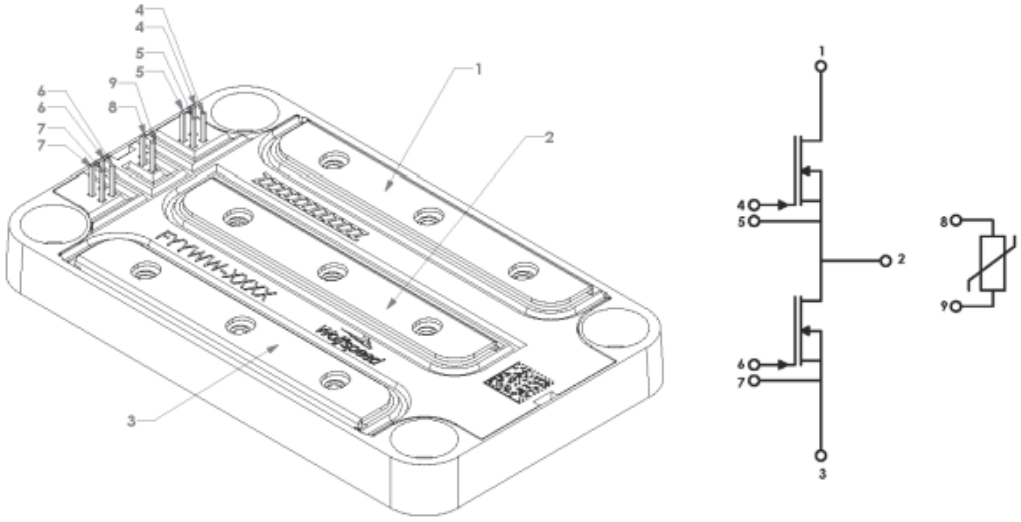

Figure 27. CREE/Wolfspeed 'HM3' Module Schematic and Pinout [13]

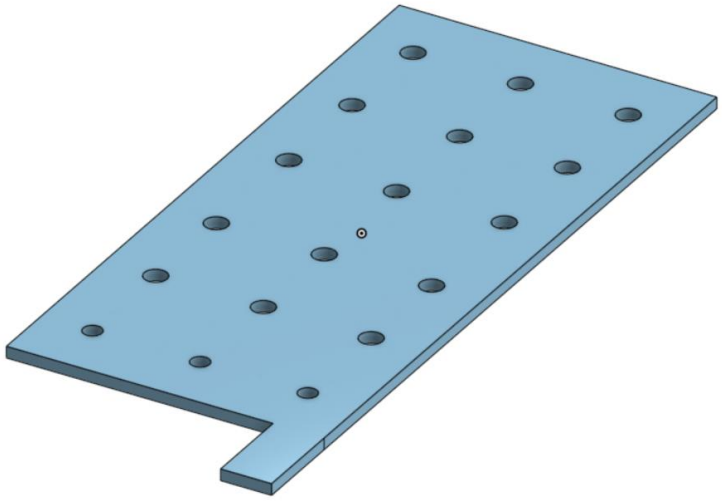

Figure 28. Prototype Busbar Work – Ground Layer for Single Phase FCI Design

From Figure 27 and the circuit schematic of a three-level FCI in mind as shown in Figure 9, a total of 4 switches are required for each phase, or 2 modules. For the ground connection, smaller holes slightly larger than M4 located at the last row of the layer. Midsized holes serve as clearance for the threads of screws for other layers.

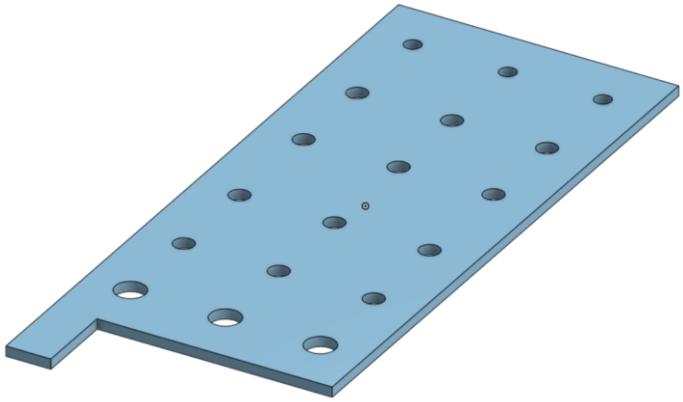

Figure 29. Prototype Busbar Work – Power Layer for Single Phase FCI Design

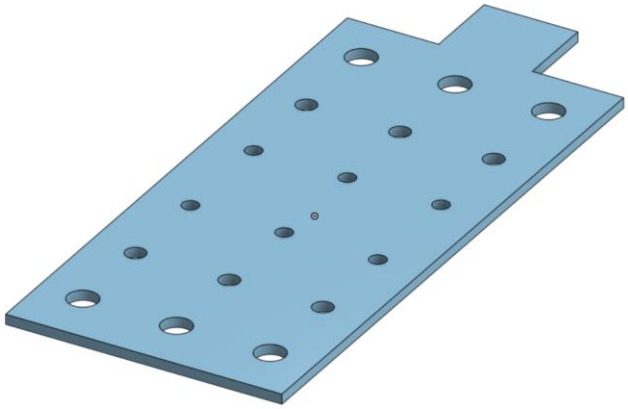

Figure 30. Prototype Busbar Work – Midpoint Layer for Single Phase FCI Design

For the power layer, smaller holes sized at M4 are made towards the first row. Larger holes sized at around M8 are made at row 6 to serve as clearance of screw heads made on the ground layer. This is seen in Figure 29. In Figure 30, large holes sized at M8 are located at rows 1 and 6 to serve as clearance for the ground and power layer. Smaller holes sized at M4 are located at rows 3 and 4 for the midpoint connection. Midsized holes sized at M5 to M6 serve as clearance for screw threads.

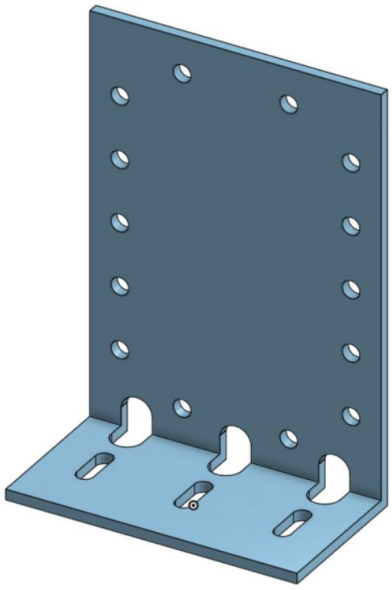

Figure 31. Prototype Busbar Work – Capacitor Layer for Single Phase FCI (1-Half)

The final layer serves as the capacitor layer. It sits on top of all other layers and holds 10 capacitors within the outer ring shown in Figure 31. A larger more cylinder-shaped hole is along the bend of the final layer. This is to serve as clearance to the midpoint layer. The smaller cylinder-shaped hole serves as the final connection to the inverter.

A cylinder-shaped hole was made to give maneuverability to the capacitors as a fail-safe. The total weight of the bus bar work that uses 0.1 in thickness aluminum and fiberglass insulation for the three-level FCI using the 'HM3' family modules comes out to be approximately 630g.

3.7: *Weight and Cost*

The weight of the prototype FCI for a three-phase system is provided in Table I.

Table I: Overall Weight of 'HM3' Family 3-level FCI Design.

Selection	**Part Number**	**Weight**	**Quantity**	**Total Weight**
Switches	CAS480M12HM3 OR CAB760M12HM3	180g	6	1080g
Gate Drivers	CGD1700HB3P-HM3	65g	6	390g
Diff. Trans.	CGD12HB00D	25g	6	150g
Flying Caps	L1GN30G204KA10	10g	30	300g
Heat Sink	688552F00000G	278g	3	835g
DSP	TMS320F2837XD	50g	1	50g
Bus Bar Layers	-	630g	3	1890g
Current Sensors	HAC 400-S	70g	2	140g
				4835g

The total cost of the 'HM3' family design is shown in tables II and III.

Table II: Total Cost of Prototype Inverter Design using 'CAB760M12HM3'

Selection	**Part Number**	**Cost**	**Quantity**	**Total Cost**
Switches	CAB760M12HM3	$2748.75	6	$16492.5
Gate Drivers	CGD1700HB3P-HM3	$327.5	6	$1965
Diff. Trans.	CGD12HB00D	$37.50	6	$225
Thermal Adhesive	GL-60-10	$70.95	1	$70.95
Flying Caps.	L1GN30G204KA10	$235.78	30	$7073.4
Heat Sink	688552F00000G	$27.76	1	$27.76
Busbar Work	-	$1100	1	$1100
Current Sensors	HAC 400-S	$93.10	2	$186.20
				$27140.81

Table III: Total Cost of Prototype Inverter Design using 'CAS480M12HM3'

Selection	**Part Number**	**Cost**	**Quantity**	**Total Cost**
Switches	CAS480M12HM3	$2,157.73	6	$12946.38
Gate Drivers	CGD1700HB3P-HM3	$327.5	6	$1965
Diff. Trans.	CGD12HB00D	$37.50	6	$225
Thermal Adhesive	GL-60-10	$70.95	1	$70.95
Flying Caps.	L1GN30G204KA10	$235.78	30	$7073.4
Heat Sink	688552F00000G	$27.76	1	$27.76
Fans	109R0605M401	$8.56	3	$25.68

DSP	TMS320F2837XD	$40.55	1	$40.55
Busbar Work	-	$1100	1	$1100
Current Sensors	HAC 400-S	$93.10	2	$186.20
				$23660.92

Additional weights are costs were made for the 'XM3' Three-Level FCI and the 'HM3' Four-Level design just incase they were to be pursued in the near future. This is shown in Table IV and V.

Table IV: Overall Weight of 'XM3' Family 3-Level FCI Design

Selection	**Part Number**	**Weight**	**Quantity**	**Total Weight**
Switches	CAB450M12XM3	175g	6	1050g
Gate Drivers	CGD12HBXMP	40g	6	240g
Diff. Trans.	CGD12HB00D	25g	6	150g
Flying Caps	L1GN30G204KA10	10g	30	300g
Heat Sink	688552F00000G	134.1g	3	402.3g
DSP	TMS320F2837XD	50g	1	50g
Bus Bar Layers	-	315g	3	945g
Current Sensors	HAC 400-S	70g	2	140g
				3277.3g

To pursue a four-level FCI design, custom made bus bar layers and capacitors are required in reducing the overall weight. In Figures 28-31, the busbar work spans

across the entire area of two modules. However, this is a very ineffective way to have light busbar work. For example, in the ground layer, only row 6 forms the ground connection. The rest is extra added weight to the design. By removing the extra weight, the weight of the bus bar can be reduced significantly. This may create a larger inductive loop between the power and the ground plane, so an idea is to keep the ground plane large and have the power plane eliminate its extra area.

In addition, a custom-made capacitor can used that meets the voltage and current requirements while having a lightweight design. Overall, this still forces strict weight requirements for both the bus bar work and capacitors. Table V gives an idea of how heavy the bus bars and capacitors must be to stay within the maximum weight of 5 kg.

Table V: Overall Weight of 'HM3' Family 4-level FCI Design

Selection	**Part Number**	**Weight**	**Quantity**	**Total Weight**
Switches	CAS480M12HM3 OR CAB760M12HM3	180g	9	1620g
Gate Drivers	CGD1700HB3P-HM3	65g	9	585g
Diff. Trans.	CGD12HB00D	25g	9	225g
Flying Caps	L1GN30G204KA10	10g	60	600g
Heat Sink	688552F00000G	370.67	3	1112
DSP	TMS320F2837XD	50g	1	50g
Bus Bar Layers	**Custom	330g	3	990g

Current Sensors	HAC 400-S	70g	2	140g
Cable (AWG 4, 2ft)	CF310.UL.1200.01	142g	1	142g
				5464g

Another way to pursue a 4-level FCI design is to stick with the 'XM3' family due to its smaller area, allowing a lighter heatsink to keep the design well below 5 kg as shown in Table VI. As a comment, the 'HM3' design can achieve a cooler design without the need for forced convection, but it will be a bit heavier. For the 'XM3' design, it was significantly lighter due to its compact area allowing for a lighter heatsink, but its thermal performance is reliant on forced convection. The overall weight of these designs is also assuming that any forced air cooling is external to the inverter, thus, not being apart of the power density calculations.

Table VI: Overall Weight of 'XM3' Family 4-level FCI Design

Selection	**Part Number**	**Weight**	**Quantity**	**Total Weight**
Switches	CAB450M12XM3	175g	9	1575g
Gate Drivers	CGD12HBXMP	40g	9	360g
Diff. Trans.	CGD12HB00D	25g	9	225g
Flying Caps	L1GN30G204KA10	10g	60	600g
Heat Sink	688552F00000G	178.8g	3	536.4g
DSP	TMS320F2837XD	50g	1	50g
Bus Bar Layers	-	350	3	1050g

Current Sensors	HAC 400-S	70g	2	140g
Cable (AWG 4, 2ft)	CF310.UL.1200.01	142g	1	142g
				4978.4g

3.8: *Power Density*

Numerous designs were explored, and a prototype was made using the 'HM3' modules. The power density for each design is determined by assuming an output power of 250 kW. The prototype's power density is shown below for an *idealistic* case. The more *realistic* results are highlighted in green:

- Power Density of 'HM3' 3-Level FCI Design: 250 kW/4.84 kg = 51.653 kW/kg
    - This design is the current prototype that was built.
    - The power density can easily be increased through custom made parts.
    - The power density of the prototype can be improved by developing more customized bus bar work and capacitors to further reduce the weight, the expected power density is around 55-58 kW/kg considering a human error factor.

The power density of the 'XM3' modules implementing a 3-level FCI design is shown below:

- Power Density of 'XM3' 3-Level FCI Design: 250 kW/3.3 kg = 75 kW/kg
    - The power density of this design is surprisingly quite high.
    - This is due to how much smaller the area of the 'XM3' modules are compared to the 'HM3' ones.
    - The smaller area allows for a smaller area heatsink and busbar work for the same thermal and electrical performance, significantly reducing the weight.
    - This allows for massive headroom for error and additional things to be added such as an enclosure if this design were to be pursued in the future.
    - The only downside is that given the voltage/current requirements, this design does require at least 400 LFM airflow to keep the junction temperature below its maximum rated if the bare minimum area heatsink is used.
    - A larger heatsink can be used to decrease the temperature of the inverter at the cost of the overall weight.
    - Realistically, fans should be apart of the weight of the inverter, resulting in a power density of 65 kW/kg. With a human error factor, the expected power density of this design should be around 60 kW/kg.

The power density of the 4-level FCI design is shown below:

- Power Density of 'HM3' 4-Level FCI Design: 250 kW/5.46 kg = 45.79 kW/kg

    - This design can only be achieved through custom made bus bar
    - Can be improved through custom made capacitors
    - This design is very strict
- Power Density of ‘XM3’ 4-Level FCI Design: 250 kW/4.978 kg = 50.22 kW/kg
    - This design can be achieved through the current prototype components.
    - The power density can be increased through custom made capacitors

Chapter 4: *Prototype*

4.1: *Overview*

A prototype was made using the 'HM3' module rated at 480A. An image of the prototype is shown in Figure 32.

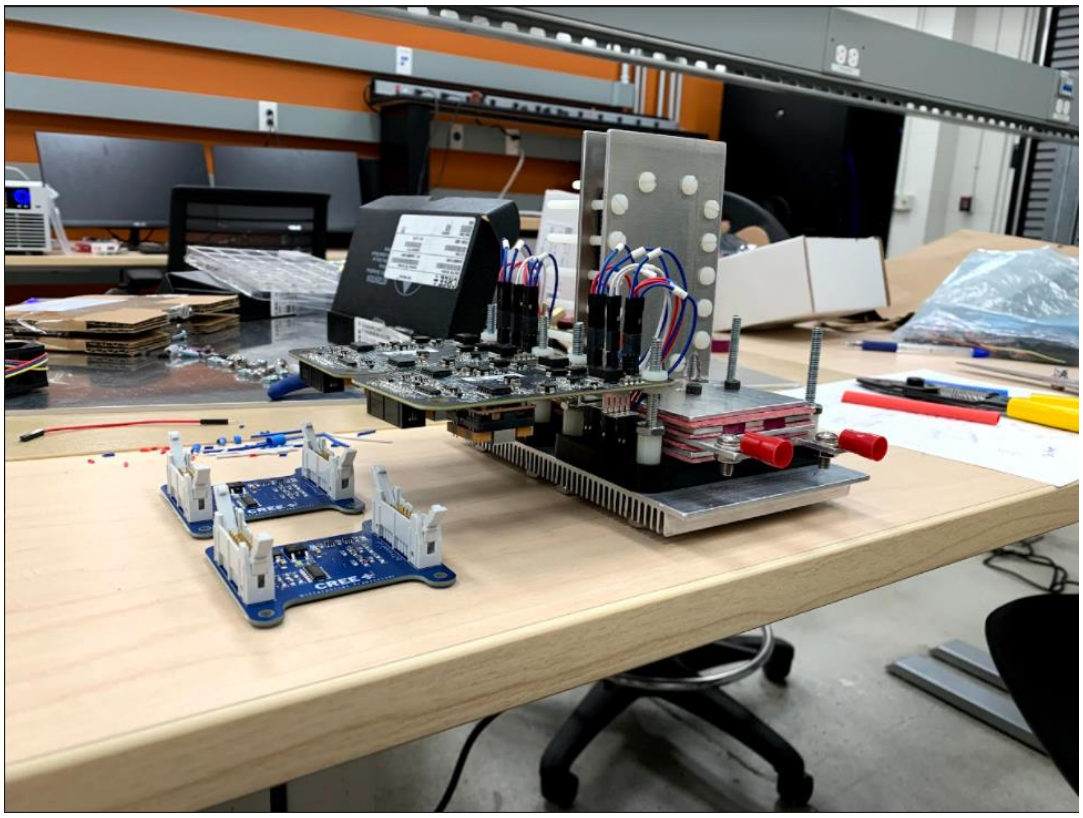

Figure 32. Physical Prototype of Single-Phase 3-Level FCI Design (Around 52 kW/kg)

The power density of the prototype is quite close to calculated in section 3.8 assuming the output power remains at 250 kW.

4.2: *Gate Driver Control*

The gate driver can be controlled with a microcontroller or a DSP. The microcontroller used for controlling the inverter is TI's LAUNCHXL-F28379D shown in Figure 33.

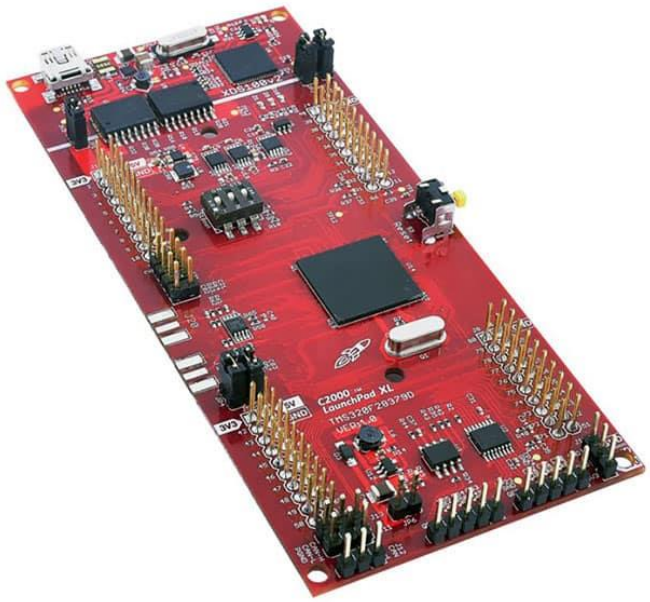

Figure 33. Microcontroller Used for Power Electronics Control Programming

To program this microcontroller, it could be programmed using C and Code Composer Studio. However, there are other methods that simplify this process. In MATLAB Simulink, a hardware addon for the C2000 processor can be installed and used to program this board. Therefore, students can use Simulink blocks to put

together a control circuit and program it into the microcontroller instead of using C. A picture of the embedded coder package addon for C2000 processors is shown in Figure 34.

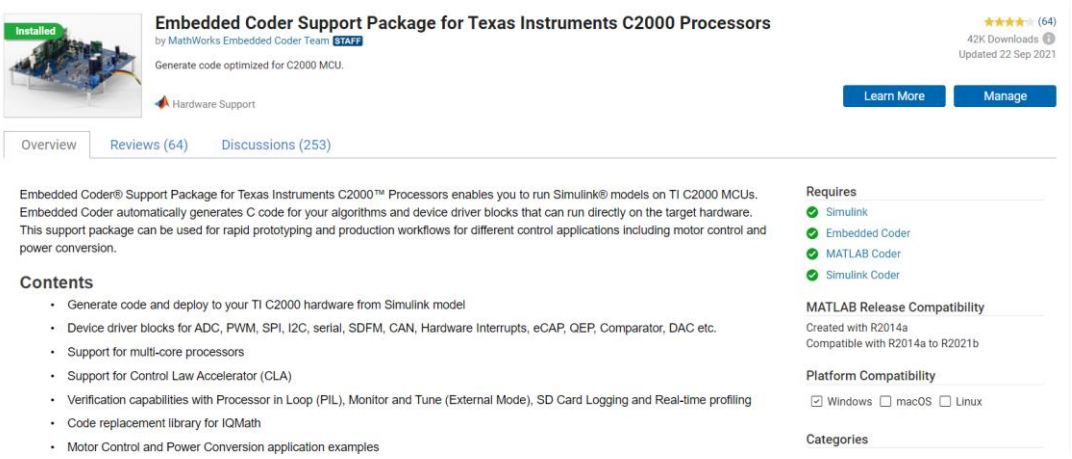

Figure 34. MATLAB Addon for TI C2000 Processors Embedded Coder Support

To implement an open-loop sine triangle modulation for the inverter design, Figure 35 displays a Simulink example of how it is done.

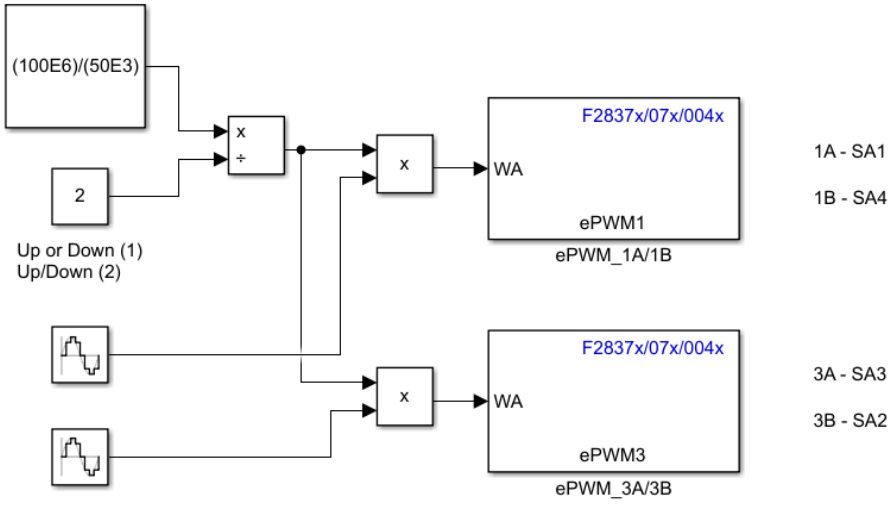

Figure 35. Simulink Implementation of PS-PWM for C2000 Programming

The ePWM blocks generate either a ramp or triangle function depending on the mode selected. For this application, the counter is selected to be Up/Down mode to generate the triangle wave. This triangle wave is compared with the incoming sine wave fed into the WA input. With a switching frequency of 50 kHz, the period of the triangle wave in clock cycles is determined by the following equation:

$$T_{period} = \frac{f_{DSP\_CLOCK}}{K_{mode} * f_{sw}}$$

where f_{DSP_CLOCK} = 100 MHz, K_{mode} = 1 (Up or Down) or 2 (Up/Down) and f_{sw} = 50 kHz. This is shown in Figure 36.

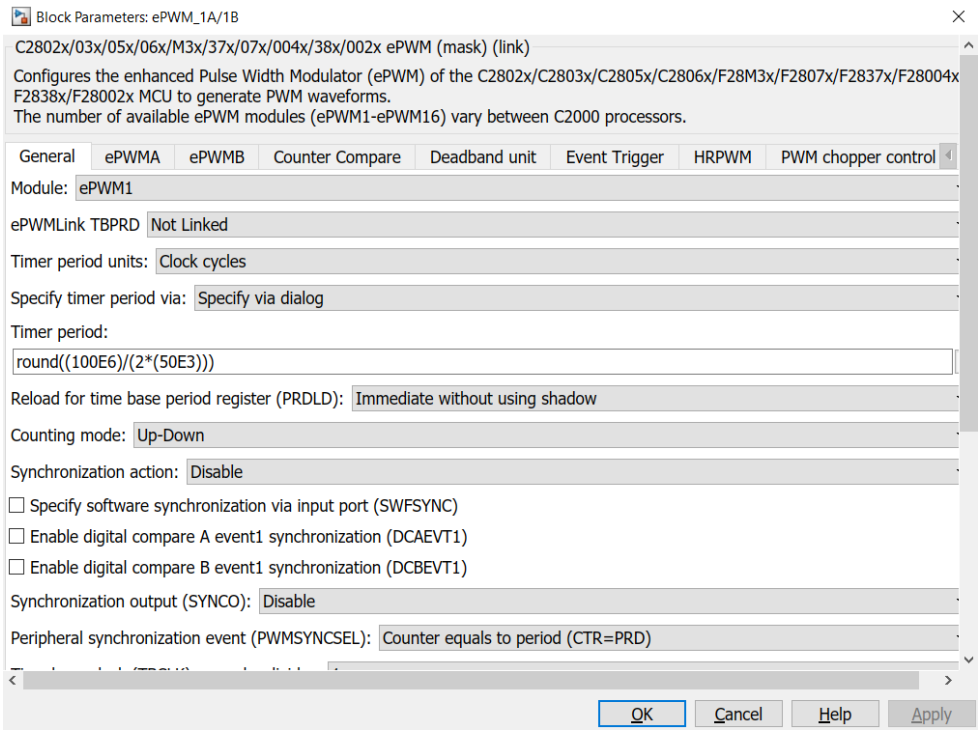

Figure 36. ePWM Settings for PS-PWM Implementation

This method can not only control the prototype inverter, but it is used for other power electronics controls. For example, a buck converter can implement a closed-loop feedback control by using a voltage and current sensor, where the ADC of the DSP can pick up both measurements for the error calculation when adjusting the duty cycle of the PWM output.

4.3: *Experimental Tests and Results*

The single-phase prototype was tested with an RL load. The resistive load is 50 Ohms, and the inductive load is 1 mH. It was tested at low voltages to verify if it was behaving properly. An oscilloscope capture of the output voltage, Vag, and the current, Ias, is shown in Figure 37. By observing the output voltage, it is indeed giving the typical three-levels. From the current, it is concluded this design is indeed inverting. The prototype implements PS-PWM with its third harmonic removed for a larger modulation index. The figure displays a test with a supply voltage of 20V. Higher voltage tests are still being conducted.

Figure 37. Oscilloscope Capture of Single-Phase Prototype Performance at Low-Voltage

4.4: *Next Setup*

The next experimental test setup involves changing out the resistive load for something that can handle the current rating. Unfortunately, the wirewound resistors being used are only rated for 2000 W, while the endgame test would like to see 83 kW per phase. The power supplies in the lab is Keysight N8930A, which have a maximum output power rating of 10 kW each. Therefore, to get a decent higher power test, the resistive load needs to be changed to something that can handle the rating. From the list of potential replacements, it was concluded that using a water heater element would be the cheapest reliable alternative. A figure of a water heater element is shown in Figure 38.

Figure 38. Water Heater Element for Higher Power Test

The water heater elements for the inverter application are rated for 5500W/240V, which is around 10.5 Ohms. Around 20 Ohms is required for the inverter prototype to reach 20 kW assuming a total of 2 power supplies are used for the test. Therefore, to satisfy the power rating and required resistance, 8 of the elements are needed, where 4 elements are connected in series connected in parallel with another 4. This setup is shown in Figure 39.

Figure 39. Water Heater Element Resistive Load for Higher Power Test

4.5: *Thermal Performance*

As experimental tests are still being performed, a thermal performance simulation was made in COMSOL to investigate how hot the inverter can get during air-cooling. In this simulation, air-cooling was assumed to be uniform instead of from one direction. The airflow was assumed to be around 400 LFM. From the simulation, the hottest section of the inverter is around 437 degK, which is around 163.85 degC. The material of the heatsink is assumed to be aluminum in the simulation, although, the actual material of the heatsink is an aluminum-based alloy. Although this is under the maximum junction temperature, the calculated junction temperature was around 120 degC. The difference in thermal performance is hypothesized to be the selected material in simulation. The simulation result in shown in Figure 40.

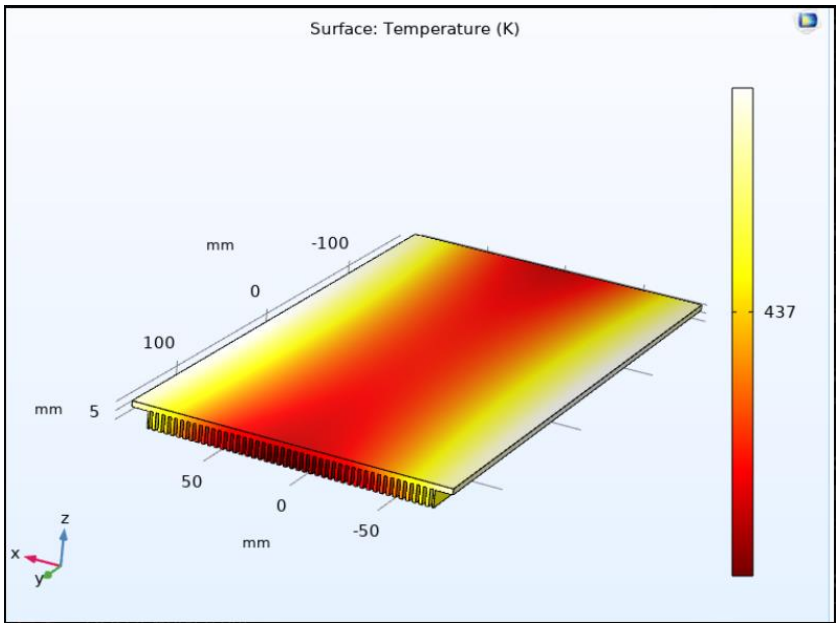

Figure 40. COMSOL Simulation of Prototype Inverter

Chapter 5: *Improvement*

5.1: *Overview*

This thesis explores numerous multilevel SiC inverter designs. For a three-level FCI topology, 55-60 kW/kg power density can be reasonably achieved. For a four-level FCI topology, a 46-52 kW/kg power density can be achieved. Although numerous designs were simulated and explored, the next steps primarily consist of verifying the thermal performance and improve on what is currently developed.

5.2: *Custom Work for 'XM3' Family*

The steps subsequent to the current design would be to optimize the bus bar work and capacitors. Currently, the bus bar work contains many layers for the required connections shown in Section 3.6. The area required to establish the necessary connections can be significantly reduced to mitigate the overall weight. Custom made capacitors with the required capacitance and voltage/current ratings can made with an optimized weight design. Figure 41, 42, and 43 displays adjusted designs made on Onshape.

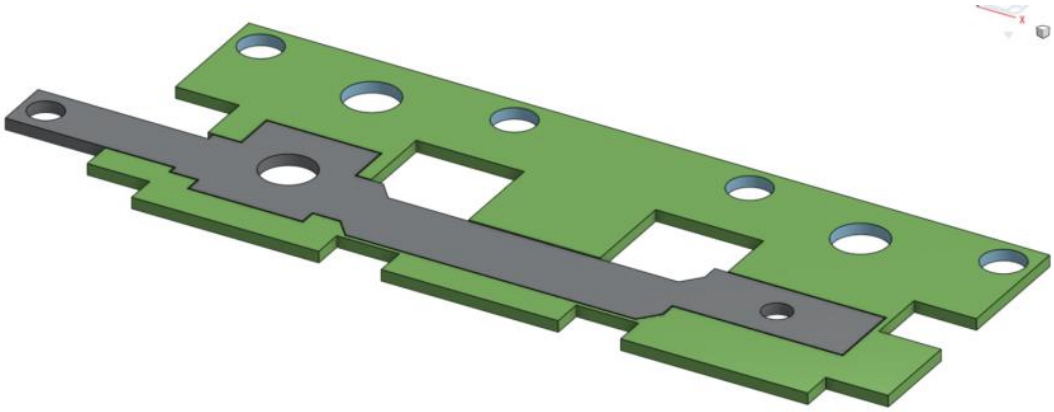

Figure 41. Adjusted Layer 1 for ‘XM3’ Family Inverter Design

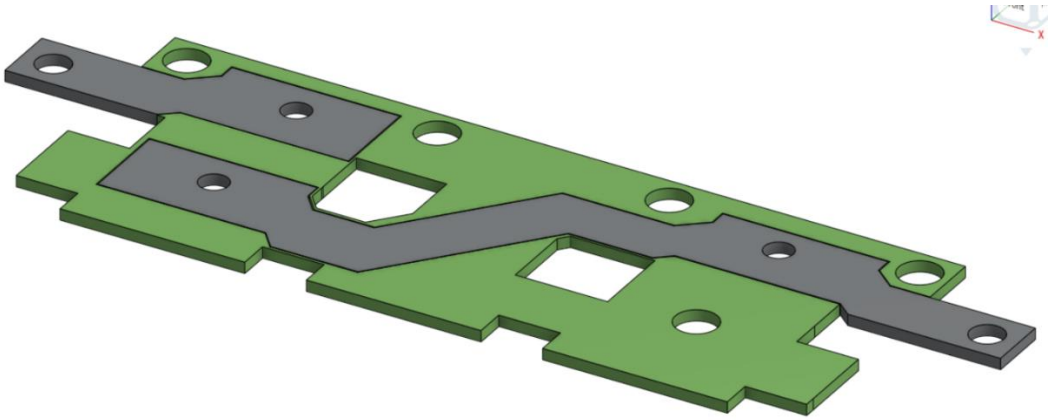

Figure 42. Adjusted Layer 2 for ‘XM3’ Family Inverter Design

Figure 43. Physical Layout of Custom Capacitor for 'XM3' Family Inverter Design

5.3: *Soft-Switching*

Although SiC devices are used in the current prototype and are known to mitigate switching losses, electromagnetic compatibility issues can still occur through hard switching. During on-off transitions in a typical hard-switching circuit, the current and voltage changes sharply, inducing switching noise and losses. In a soft-switching circuit, an LC resonant circuit is used to turn off and on switches at zero voltage or current. Due to this, soft-switching aids in reducing switching losses and noise even further as shown in Figure 44 [17].

Figure 44. Characteristics of Hard-Switching versus Soft-Switching [17]

The three-level FCI circuit can incorporate soft-switching by implementing a LC resonant circuit with three axillary switches as shown in Figure 45. A current of 32A was applied at the output to investigate the soft switching performance.

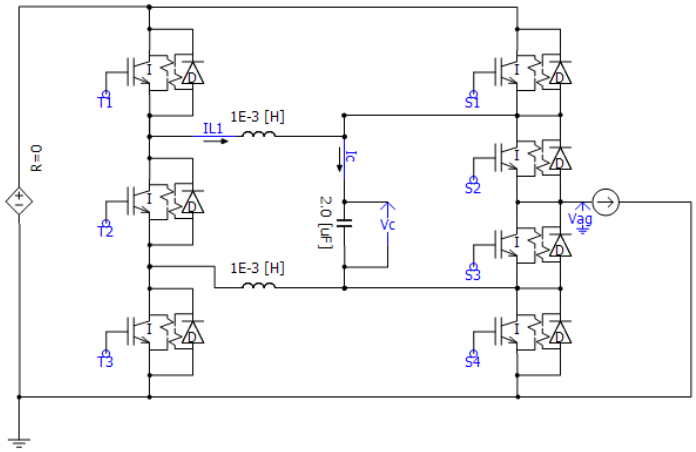

Figure 45. PSCAD Schematic of a Single-Phase Three-Level FCI Soft-Switching Topology

The switching logic for the soft-switching three-level FCI in shown in Figure 42.

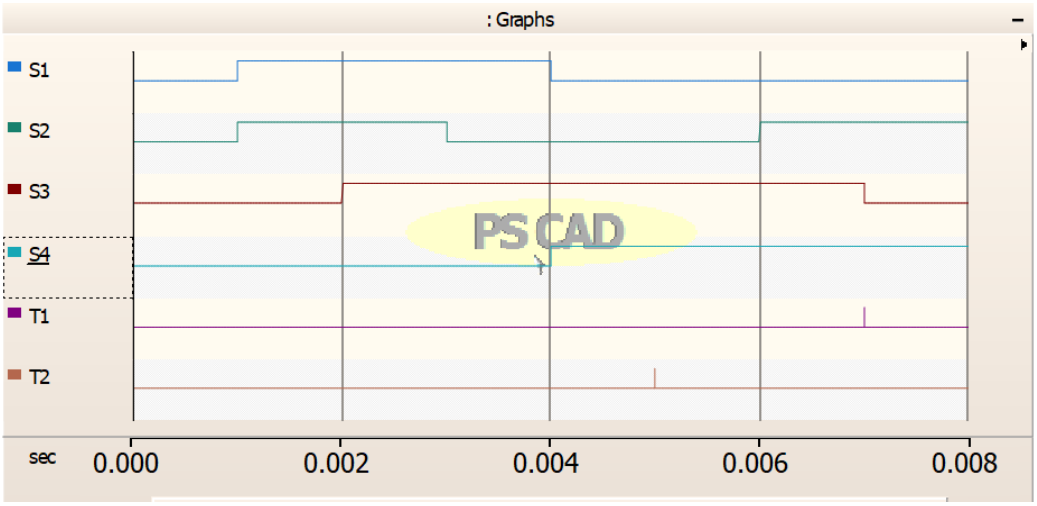

Figure 46. Soft-Switching Three-Level FCI Switching Logic

From the iterating through all possible switching states for a large current positive cycle, parameters such as inductor current and capacitor voltage were monitored. These parameters are shown in Figures 47-50.

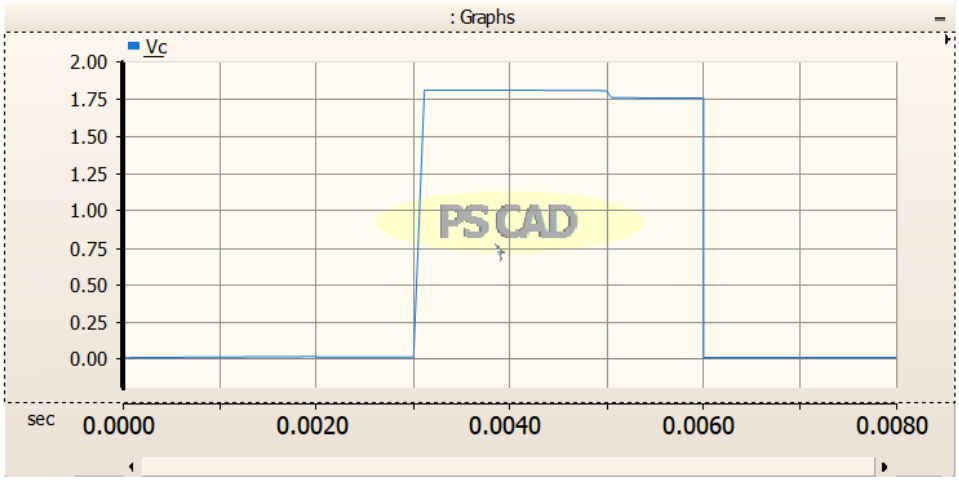

Figure 47. Capacitor Voltage during Soft-Switching

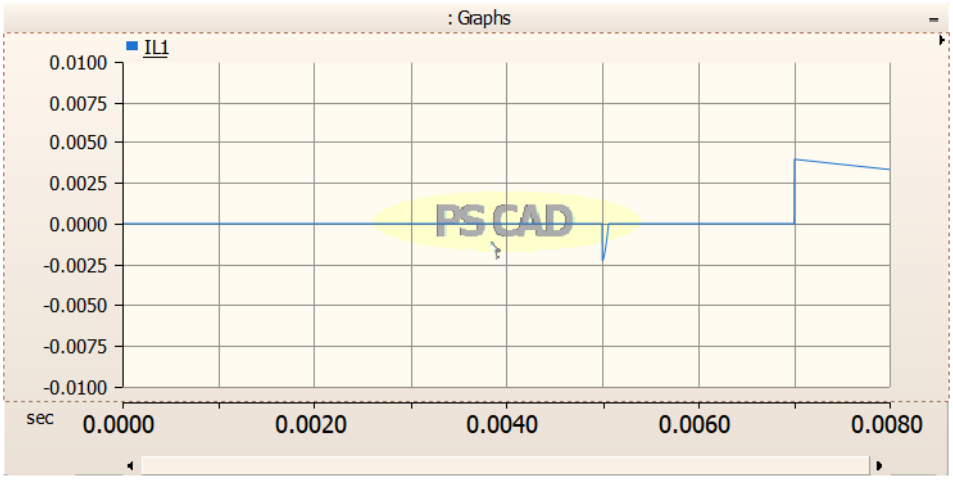

Figure 48. Top Inductor Current during Soft-Switching

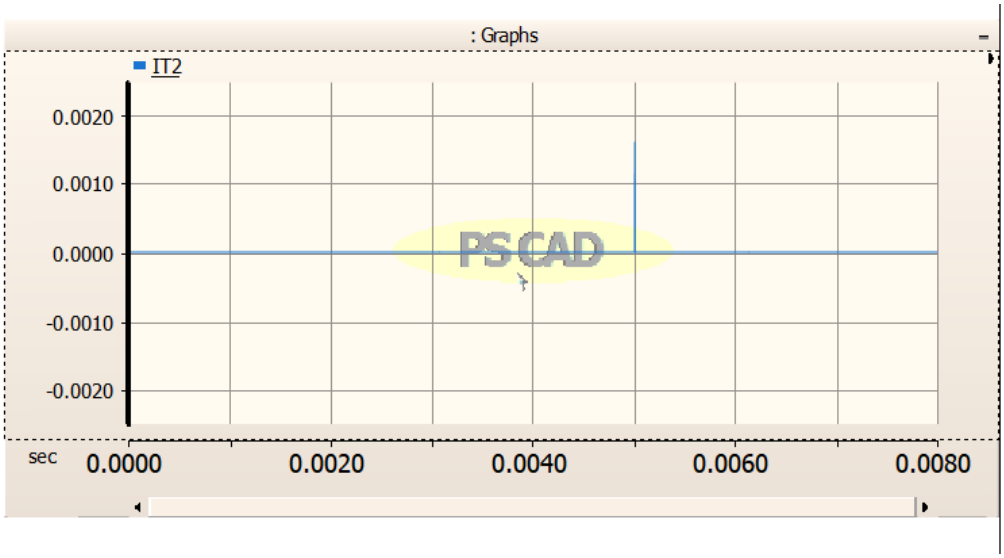

Figure 49. Current along Transistor T2 During Soft-Switching

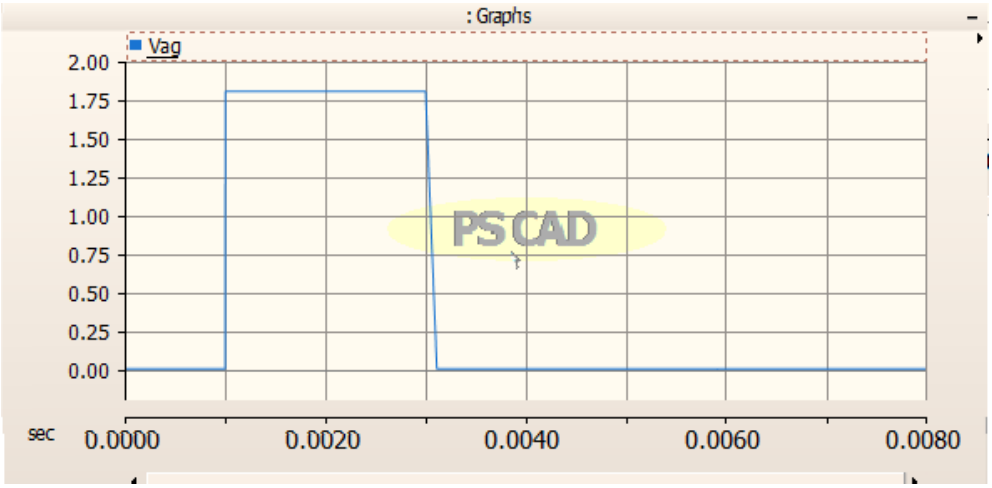

Figure 50. Output Voltage, Vag, During Soft-Switching

If soft-switching shows promise and can remain within the power density requirement, soft-switching needs to be further invested at negative current and lower values of current.

As a general overview, assuming inductors weight around 300g each and auxiliary switches weight a measly 6g, the expected power density range incorporating soft-switching is 39.2-50.5 kW/kg.

5.4: *Liquid-Cooling*

The current prototype aims to implements air cooling to keep the junction temperature during full load below its maximum rated of 175 degC. The benefits of liquid cooling is quite self-explanatory. Liquid cooling is significantly more efficient than air cooling, which will allow the operating temperature of the modules to be significantly lower versus air cooling, elongating the lifetime of the devices. A company by the name of Microcool makes double-sided coldplates that are specifically designed for high heat flux of SiC, allowing for very low thermal resistance, low pressure drop, and balanced parallel flow. An example of a double-sided coldplate for 'HM3' and 'XM3' family modules is shown in Figure 51 [18] [19]. Provided these designs are double sided, it would be the perfect steppingstone for a more polished future design. A slight downside is the weight. The coldplate weighs around double the weight of the heatsink. If soft-switching is not implemented, the hard switching designs can sacrifice some power density for the sake of significantly better thermal performance. If the coolant section is not apart of power density calculations, similar to how weight of fans is not included for the air-cooling alternative, it would be beneficial to look into.

Figure 51. Microcool Coldplates for ‘XM3’ and ‘HM3’ Family Modules [18] [19].

It would be wise to keep the coolant temperature around room temperature instead of cyro. According to paper [20], SiC devices tend to become very inefficient at lower temperatures as shown in Figure 52. In addition, in Figure 21, the modules have a minimum operating temperature of -40 degC.

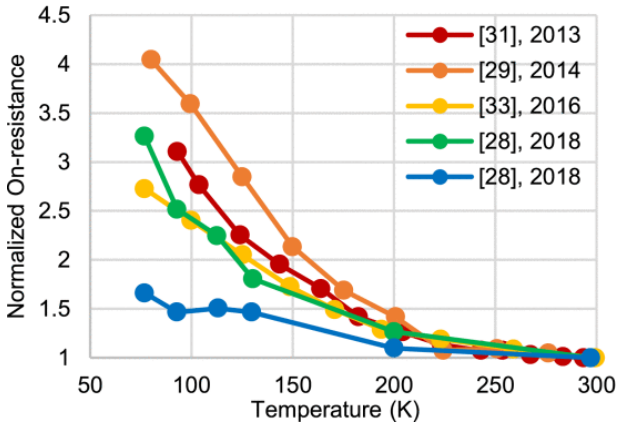

Figure 52. On-Resistance vs Temperature of SiC Devices [20].

Liquid cooling would be another topic to investigate. Although it would decrease power density due to the weight of the coldplate, the thermal performance of the modules would allow a longer life-time design.

5.5: *Best-Case Power Density*

Power density was recalculated to reconsider custom bus-bars, considering both air cooling and liquid cooling alternatives. These results are shown in Tables VII-X.

Table VII. 'HM3' Family Design – Air Cooling BEST Case

Selection	**Part Number**	**Weight**	**Quantity**	**Total Weight**
Switches	CAS480M12HM3 OR CAB760M12HM3	180g	6	1080g
Gate Drivers	CGD1700HB3P-HM3	65g	6	390g
Diff. Trans.	CGD12HB00D	25g	6	150g
Flying Caps	L1GN30G204KA10	10g	30	300g
Heat Sink	688552F00000G	278g	3	835g
DSP	TMS320F2837XD	50g	1	50g
***Custom* Bus Bar Layers**	approx.	330g	3	990g
Current Sensors	HAC 400-S	70g	2	140g
Cable (AWG 4, 2ft)	CF310.UL.1200.01	142g	1	142g
				4077g

Table VIII. ‘XM3’ Family Design – Air Cooling BEST Case

Selection	**Part Number**	**Weight**	**Quantity**	**Total Weight**
Switches	CAB450M12XM3	175g	6	1050g
Gate Drivers	CGD12HBXMP	40g	6	240g
Diff. Trans.	CGD12HB00D	25g	6	150g
Flying Caps	L1GN30G204KA10	10g	30	300g
Heat Sink	688552F00000G	134.1g	3	402.3g
DSP	TMS320F2837XD	50g	1	50g
***Custom* Bus Bar Layers**	approx.	315g	3	945g
Current Sensors	HAC 400-S	70g	2	140g
Cable (AWG 4, 2ft)	CF310.UL.1200.01	142g	1	142g
				3419.3g

Table IX. ‘HM3’ Family Design – Liquid Cooling BEST Case

Selection	**Part Number**	**Weight**	**Quantity**	**Total Weight**
Switches	CAS480M12HM3 OR CAB760M12HM3	180g	6	1080g

Gate Drivers	CGD1700HB3P-HM3	65g	6	390g
Diff. Trans.	CGD12HB00D	25g	6	150g
Flying Caps	L1GN30G204KA10	10g	30	300g
Coldplate	CP4009D	500g	3	1500g
DSP	TMS320F2837XD	50g	1	50g
***Custom* Bus Bar Layers**	approx.	330g	3	990g
Current Sensors	HAC 400-S	70g	2	140g
Cable (AWG 4, 2ft)	CF310.UL.1200.01	142g	1	142g
				4742g

Table X. 'XM3' Family Design – Liquid Cooling BEST Case

Selection	**Part Number**	**Weight**	**Quantity**	**Total Weight**
Switches	CAB450M12XM3	175g	6	1050g
Gate Drivers	CGD12HBXMP	40g	6	240g
Diff. Trans.	CGD12HB00D	25g	6	150g
Flying Caps	L1GN30G204KA10	10g	30	300g
Coldplate	CP4012D	288g	3	863g
DSP	TMS320F2837XD	50g	1	50g

***Custom* Bus Bar Layers**	approx.	315g	3	945g
Current Sensors	HAC 400-S	70g	2	140g
Cable (AWG 4, 2ft)	CF310.UL.1200.01	142g	1	142g
				3880g

The resulting BEST CASE power density is as follows:

‘HM3’ – Air Cooling: 61.32 kW/kg

‘XM3’ – Air Cooling: 73.1 kW/kg

‘HM3’ – Liquid Cooling: 52.72 kW/kg

‘XM3’ – Liquid Cooling: 64.43 kW/kg

5.6: Exploring the ‘XM3’ Family

Since the ‘XM3’ family provides the best power density provided its smaller area in comparison to the ‘HM3’ family for the same thermal performance in both air and liquid cooling conditions, it was further investigated, and its physical design was mapped out in more detail. A single-phase layout was mapped out in Onshape with the custom-made bus bar and capacitor to get a better idea of how it should look like.

The length turns out to be 183 cm. The width is 110cm. The height being around 50 cm. This is shown in Figure 53.

\

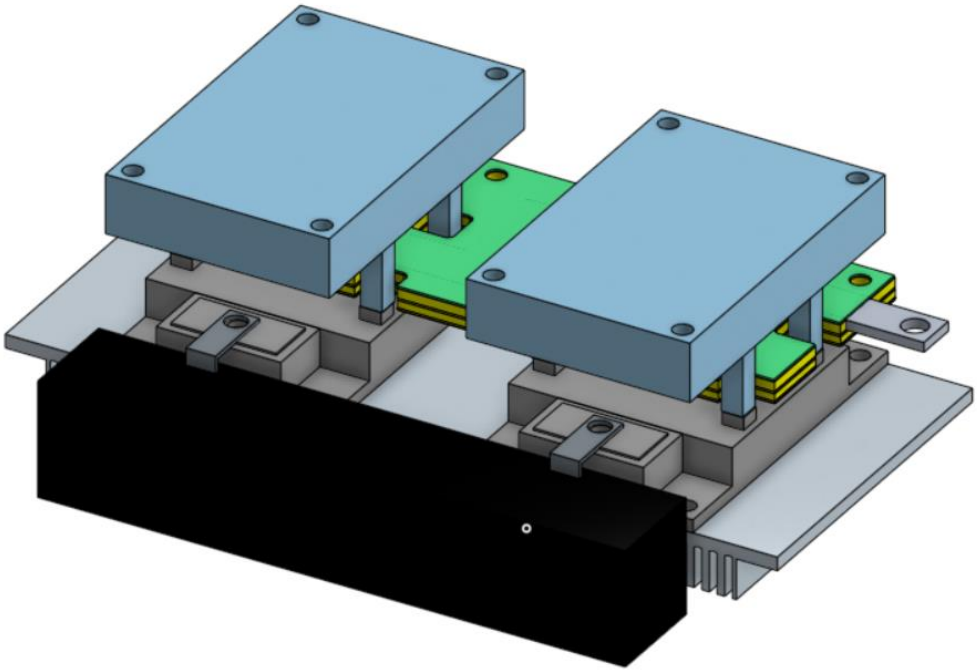

Figure 53. Onshape Single-Phase Layout of ‘XM3’ Family Implementing 3-Level FCI

Chapter 6: *Conclusion*

Overall, this thesis explored numerous inverter topologies to satisfy the power density requirement of 50 kW/kg. The best devices selected are the 'HM3' and 'XM3' family modules from CREE/Wolfspeed. Both air and liquid cooling were explored to identify the best possible options. From the calculations made, it is identified that the best-case power density of the 'HM3' and 'XM3' family that implements hard switching are:

Best Case 'HM3' Power Density Range: 52.72 – 61.32 kW/kg

Best Case 'XM3' Power Density Range: 64.43 – 73.1 kW/kg

A different type of inverter was explored as well. An NPC (Neutral-Point Clamped) inverter was investigated, and its electrical performance rivaled the FCI. The downside of using an NPC for a high-power density design is the weight of the power diodes. The best comparison between an NPC and a FCI is the power diode versus capacitor. Capacitors designed for high power density applications are lighter weight than power diodes. A four-level FCI was explored to identify whether power density can be maintained while improving losses. The power density ranges from 46-52 kW/kg depending on the selected module.

Soft switching was also investigated to improve switching losses and improve electromagnetic capability. By implementing an LC resonance with a couple switches, soft-switching can be achieved in a three-level FCI. Unfortunately, due to

the number of inductors required and auxiliary switches, the power density incorporating soft-switching is expected to be in the range of 39.2 – 50.4 kW/kg.

Given the best-case power density being a bit above the minimum required, it was concluded that a three-level FCI with hard-switching will offer the best electrical and thermal performance at the lightest weight possible. Technically, air-cooling would provide the best power density provided that heatsinks are generally lighter than coldplates. However, this will not result in a longer lifetime design since in air cooling, the modules will be constantly operating within 90-120 degC. In a liquid cooled design, the modules will be expected to operate around room temperature, significantly improving the lifetime of the design.

A single-phase prototype was made using the 'HM3' modules. The expected power density of the prototype is around 53 kW/kg, close to the calculated 55-60 kW/kg range for the 'HM3' design. Experimental tests were performed to get a better idea of the electrical and thermal performance.

Improvements were identified and explored on Onshape. A future design that maximizes the power density incorporates the 'XM3' modules and custom-made bus bar and capacitors. This will be explored further as I work on my Ph.D for the upcoming years. The aim is to incorporate the design into the entire power train for an all-electric aircraft.

Bibliography

[1] Boechler, et. al, Primary energy, Sept. 2021, [online] Available: https://energyeducation.ca/encyclopedia/Primary_energy

[2] Rogelj, J., den Elzen, M., Höhne, N. et al. Paris Agreement climate proposals need a boost to keep warming well below 2 °C. Nature 534, 631–639 (2016). [online] Available: https://doi.org/10.1038/nature18307

[3] Virginia McConnell and Benjamin Leard, Progress and Potential for Electric Vehicles to Reduce Carbon Emissions, Dec. 2020, [online] Available: https://www.rff.org/publications/reports/potential-role-and-impact-evs-us-decarbonization-strategies/

[4] E. Apostolaki-Iosifidou, M. Pruckner, S. Woo and T. Lipman, "Electric Vehicle Charge Management for Lowering Costs and Environmental Impact," 2020 IEEE Conference on Technologies for Sustainability (SusTech), 2020, pp. 1-7, [online]. https://ieeexplore.ieee.org/abstract/document/9150524

[5] Stephens, Tim, UCSC engineers developing all-electric power train for future aircraft, Sept. 2020, [online] https://news.ucsc.edu/2020/09/electric-aircraft.html

[6] A. K. Misra, Technical Challenges and Barriers Affecting Turbo-Electric and Hybrid Electric Aircraft Propulsion, Jun. 2017, [online] Available: https://ntrs.nasa.gov/archive/nasa/casi.ntrs.nasa.gov/20180004252.pdf

[7] Aviation-Class Synergistically Cooled Electric Motors With Integrated Drives (ASCEND) Funding Opportunity No. DE-FOA-0002238, Jun. 2020, [online] Available: https://arpa-e-foa.energy.gov/FileContent.aspx?FileID=5b0e42aa-1c55-44a1-a4b3-4c4940a6af12

[8] K. Yamaguchi, K. Katsura and T. Yamada, "Comprehensive evaluation and design of SiC-Based high power density inverter, 70kW/liter, 50kW/kg," 2016 IEEE 8th International Power Electronics and Motion Control Conference (IPEMC-ECCE Asia), 2016, pp. 1-7, [online] https://ieeexplore.ieee.org/document/7512253

[9] S. Yin, K. J. Tseng, R. Simanjorang, Y. Liu and J. Pou, "A 50-kW High-Frequency and High-Efficiency SiC Voltage Source Inverter for More Electric Aircraft," in IEEE Transactions on Industrial Electronics, vol. 64, no. 11, pp. 9124-9134, Nov. 2017, [online] https://ieeexplore.ieee.org/document/7906552

[10] A. M. Y. M. Ghias, J. Pou, M. Ciobotaru and V. G. Agelidis, "Voltage-Balancing Method Using Phase-Shifted PWM for the Flying Capacitor Multilevel Converter," in IEEE Transactions on Power Electronics, vol. 29, no. 9, pp. 4521-4531, Sept. 2014, [online] https://ieeexplore.ieee.org/document/6628025

[11] R. Sarker, "Phase Disposition PWM (PD-PWM) Technique to Minimize WTHD from a Three-Phase NPC Multilevel Voltage Source Inverter," 2020 IEEE 1st International Conference for Convergence in Engineering (ICCE), 2020, pp. 220-224, [online] https://ieeexplore.ieee.org/document/9290697

[12] 2-Channel Differential Transceiver, Wolfspeed, Jun. 2019, [online] https://assets.wolfspeed.com/uploads/2020/12/CGD12HB00D.pdf

[13] CAB760M12HM3: 1200V, 760A All-Silicon Carbide High Performance, Switching Optimized, Half-Bridge Module, Wolfspeed, May 2020, [online] https://assets.wolfspeed.com/uploads/2020/12/CAB760M12HM3.pdf

[14] Datasheet: Extrusion Profile 68855, Aavid Thermalloy, Aug. 2017, [online] https://media.digikey.com/pdf/Data%20Sheets/Nuventix%20PDFs/68855_Datasheet.pdf

[15] CAS480M12HM3: 1200V, 480A All-Silicon Carbide High Performance, Switching Optimized, Half-Bridge Module, Wolfspeed, May 2020, [online] https://assets.wolfspeed.com/uploads/2020/12/CAS480M12HM3.pdf

[16] CAB450M12XM3: 1200V, 450A All-Silicon Carbide Conduction Optimized, Half-Bridge Module, Wolfspeed, May 2019, [online] https://assets.wolfspeed.com/uploads/2020/12/CAS480M12HM3.pdf

[17] Please explain hard switching and soft switching using IGBTs, Toshiba, 2021, [online] https://toshiba.semicon-storage.com/us/semiconductor/knowledge/faq/mosfet_igbt/igbt-012.html

[18] CP4009D, Wieland Microcool, 2019, [online] https://www.microcooling.com/wp-content/uploads/2021/03/CP4009D-data-sheet.pdf

[19] CP4012D, Wieland Microcool, 2019, [online] https://www.microcooling.com/wp-content/uploads/2021/04/CP4012D-data-sheet-.pdf

[20] H. Gui et al., "Review of Power Electronics Components at Cryogenic Temperatures," in IEEE Transactions on Power Electronics, vol. 35, no. 5, pp. 5144-5156, May 2020, [online] https://ieeexplore.ieee.org/document/8854889

[21] C. Krause, O. Wasynczuk, S.D. Sudhoff, and S.D. Pekarek, Analysis of Electric Machinery and Drive Systems, Third Edition, IEEE Press, 2013